

# The Problem of Multiple Solutions in Area Navigation and Computed Centerline Operations with the Microwave Landing System

By

F. D. Powell

August 1991

Prepared for

Deputy Program Director  
Airspace Management SPO  
Electronic Systems Division  
Air Force Systems Command  
United States Air Force  
Hanscom Air Force Base, Massachusetts



Approved for public release;  
distribution unlimited

Project No. 5420  
Prepared by  
The MITRE Corporation  
Bedford, Massachusetts  
Contract No. F19628-89-C-0001

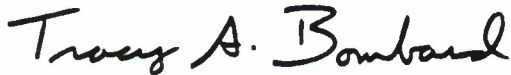
ADA242757

When U.S. Government drawings, specifications or other data are used for any purpose other than a definitely related government procurement operation, the government thereby incurs no responsibility nor any obligation whatsoever; and the fact that the government may have formulated, furnished, or in any way supplied the said drawings, specifications, or other data is not to be regarded by implication or otherwise as in any manner licensing the holder or any other person or conveying any rights or permission to manufacture, use, or sell any patented invention that may in any way be related thereto.

Do not return this copy. Retain or destroy.

### REVIEW AND APPROVAL

This technical report has been reviewed and is approved for publication.



TRACY A. BOMBARD, 1LT, USAF  
MMLSA Program Manager

FOR THE COMMANDER



JEFFREY H. THURSTON, GM-15  
Deputy Program Director  
Airspace Management SPO

# REPORT DOCUMENTATION PAGE

Form Approved  
OMB No. 0704-0188

Public reporting burden for this collection of information is estimated to average 1 hour per response, including the time for reviewing instructions, searching existing data sources, gathering and maintaining the data needed, and completing and reviewing the collection of information. Send comments regarding this burden estimate or any other aspect of this collection of information, including suggestions for reducing this burden, to Washington Headquarters Services, Directorate for Information Operations and Reports, 1215 Jefferson Davis Highway, Suite 1204, Arlington, VA 22202-4302, and to the Office of Management and Budget, Paperwork Reduction Project (0704-0188), Washington, DC 20503.

1. AGENCY USE ONLY (Leave blank)		2. REPORT DATE August 1991	3. REPORT TYPE AND DATES COVERED Final	
4. TITLE AND SUBTITLE The Problem of Multiple Solutions in Area Navigation and Computed Centerline Operations with the Microwave Landing System			5. FUNDING NUMBERS F19628-89-C-0001 5420	
6. AUTHOR(S) Powell, Frederic D.				
7. PERFORMING ORGANIZATION NAME(S) AND ADDRESS(ES) The MITRE Corporation Burlington Road Bedford, MA 01730			8. PERFORMING ORGANIZATION REPORT NUMBER  MTR-11023	
9. SPONSORING/MONITORING AGENCY NAME(S) AND ADDRESS(ES) Deputy Program Director, Airspace Management SPO (ESD/TG) Electronic Systems Division, AFSC Hanscom AFB, MA 01731-5000			10. SPONSORING/MONITORING AGENCY REPORT NUMBER  ESD-TR-91-213	
11. SUPPLEMENTARY NOTES				
12a. DISTRIBUTION / AVAILABILITY STATEMENT  Approved for public release; distribution unlimited.			12b. DISTRIBUTION CODE	
13. ABSTRACT (Maximum 200 words) In normal geometries of siting of the ground units, the Microwave Landing System (MLS) observations in the avionics of azimuth and elevation angles plus slant range from a Distance Measuring Equipment (DME) transponder yield a unique solution for the aircraft location. However, for some unconventional geometries of the ground units in a very few, preexisting installations, these observations can be consistent with two solutions for aircraft location within the MLS coverage volume. It appears that the basic MLS concept has not dealt with this multiple solutions situation, which is possible within the present international agreements. This report shows that the MLS avionics position reconstruction algorithms, which determine the aircraft location in Cartesian coordinates and are essential in area navigation, computed centerline approach, and ground operations such as deceleration and turnoff, cannot from internal data tell which of the two solutions is true and which is false. The problem can be avoided by new constraints on the permitted sites for the MLS ground units, by restrictions on the aircraft flight paths, or by Kalman filters or equivalents in the avionics. These constraints, restrictions, and filters, are defined. The first option, of further constraining the siting of the DME relative to the (continued)				
14. SUBJECT TERMS Ambiguous Solutions      Multiple Solutions Gauss      Newton Microwave Landing System      Position Reconstruction Algorithm			15. NUMBER OF PAGES 79	
			16. PRICE CODE	
17. SECURITY CLASSIFICATION OF REPORT Unclassified	18. SECURITY CLASSIFICATION OF THIS PAGE Unclassified	19. SECURITY CLASSIFICATION OF ABSTRACT Unclassified	20. LIMITATION OF ABSTRACT SAR	

13. azimuth antenna, is preferred for future installations; the second option may be appropriate to preexisting unconventional installations. The problem of multiple solutions within the MLS coverage cannot occur with the mobile MLS, for the azimuth antenna and the DME are physically collocated.

## ACKNOWLEDGMENTS

This document has been prepared by The MITRE Corporation under Project No. 5420, Contract No. F19628-89-C-0001. The contract is sponsored by the Electronic Systems Division, Air Force Systems Command, United States Air Force, Hanscom Air Force Base, Massachusetts, 01731-5000.

Ms. P. M. Hatzis contributed in many ways to the work reported herein, including development of the several algorithms and especially the subtle programming required to generate the results in section 4. Her work and contributions are acknowledged with a particular pleasure. Mr. Andrew Nelson offered valuable ideas, which appear in section 6, about possible uses of the Global Positioning System.

## TABLE OF CONTENTS

SECTION	PAGE
1 Introduction . . . . .	1
2 Common Elements . . . . .	3
2.1 Notation . . . . .	3
2.2 Observations . . . . .	4
2.3 Overview and Forecast . . . . .	5
3 Geometry and Multiple Solutions . . . . .	7
3.1 Conventional Geometries . . . . .	7
3.2 Unconventional Geometries . . . . .	8
3.2.1 Eight Solutions . . . . .	10
3.2.2 Four Solutions . . . . .	12
3.2.3 Two Solutions with Both in Coverage . . . . .	13
3.2.4 Velocity Vectors . . . . .	13
3.2.5 Unique Exception . . . . .	14
3.3 RNAV without Elevation Data . . . . .	15
3.4 Overview and Forecast . . . . .	15
4 Newton-Raphson Algorithm . . . . .	17
4.1 A Newton-Raphson Algorithm . . . . .	17
4.2 Errors in Initial Conditions . . . . .	21
4.2.1 Initializing Algorithms . . . . .	22
4.2.2 Observation Errors . . . . .	23
4.3 The Effects of Initialization Errors . . . . .	24
4.4 Overview of NR Algorithm Results . . . . .	28
5 Gauss-Seidel Algorithms . . . . .	31
5.1 The Gauss-Seidel Principle . . . . .	31
5.2 Solutions in Same Quadrant . . . . .	33
5.3 Solutions in Two Quadrants . . . . .	35
5.4 Overview of GS Algorithm Results . . . . .	36
6 Resolving the Multiple Solutions Problem . . . . .	39
6.1 Ground Equipments . . . . .	39
6.2 Aircraft Flight Paths . . . . .	41

SECTION	PAGE
6.3 Avionics .....	41
6.3.1 Avoidance .....	41
6.3.2 Position Data .....	42
6.3.3 Velocity Data .....	42
6.3.4 A Philosophical Comment .....	46
6.4 Overview .....	47
7 Conclusions .....	49
List of References .....	51
Appendix A      Secondary Solutions Using Tracking Filters .....	53
Appendix B      General Siting Constraints for the DME .....	61
Glossary .....	67



## LIST OF FIGURES

FIGURE		PAGE
2-1	Geometry and Notation . . . . .	3
3-1	A Conventional Siting for the Ground Units . . . . .	8
3-2	Unconventional Sitings for the Ground Units . . . . .	9
3-3	Geometry for Eight Solutions . . . . .	11
3-4	Geometry for Four Solutions with Two in Coverage . . . . .	12
3-5	Geometry for Two Solutions with Two in Coverage . . . . .	13
3-6	Velocity Vectors for Multiple Solutions . . . . .	14
3-7	Tangency Trajectory . . . . .	15
4-1	Newton-Raphson Iteration in a Single Variable . . . . .	17
4-2	Locations of Solutions and Singularities in the Symmetric NR PRA Problem . . . . .	20
4-3	Solutions and Singularities in an Unsymmetric Geometry . . . . .	21
4-4	Simple Limit Cycles and Wells of Attraction . . . . .	24
4-5	Initializations and Solutions: Symmetrical Case . . . . .	25
4-6	The Blue-Yellow Interface: Expanded . . . . .	26
4-7	Initializations and Solutions: Near-Tangency Case . . . . .	26
4-8	The Blue-Yellow Interface in Near-Tangency Case . . . . .	27
4-9	Small Downwind Displacement of DME . . . . .	27
4-10	Effect of Large Downwind Displacement of DME . . . . .	28
5-1	Unconventional Geometries for GS Algorithms . . . . .	32
6-1	DME Site Constraint for One Solution in Coverage . . . . .	39
6-2	DME Sites for One Solution in Coverage on the Ground . . . . .	40
6-3	Kalman Filter for Multiple Solutions . . . . .	45

## LIST OF TABLES

TABLE		PAGE
4-1	Performance of Initialization Algorithms . . . . .	23
5-1	Aircraft and Ground Unit Geometry: One-Quadrant Case 2 . . . . .	33
5-2	Behavior of Gaussian Algorithms at Blue Solution in One-Quadrant Case . . . . .	34
5-3	Aircraft and Ground Unit Geometry: Two-Quadrant Case 1 . . . . .	35
5-4	Behavior of Gaussian Algorithms at Blue Solution in Two-Quadrant Case . . . . .	36



## EXECUTIVE SUMMARY

The Microwave Landing System (MLS) concept uses three ground units – an azimuth antenna, an elevation antenna, and a distance measuring equipment (DME) transponder – and an appropriate avionics unit to enable a wide variety of operations. These operations include area navigation (RNAV) procedures such as down wind and multi-leg approaches, initial and intermediate approaches, curved approaches, approaches which control time to touchdown, and very short approaches suitable for helicopters or vertical takeoff vehicles, precision approach and landing, and the ground procedures of deceleration, turnoff, and taxiing. In part, the use of these new capabilities will be due to the need to maximize use of existing airports, and thus to avoid the political and economic difficulties now being observed in developing new airports. Figure ES-1 shows a conventional geometry for the ground units and the aircraft: the azimuth antenna and the DME are near the runway stop end, normally but not always collocated on the runway centerline extension; the elevation antenna is near the threshold; the approaching aircraft, with its location marked in yellow, is within the system's coverage volume, and there is only one possible solution within the MLS coverage for the aircraft location.

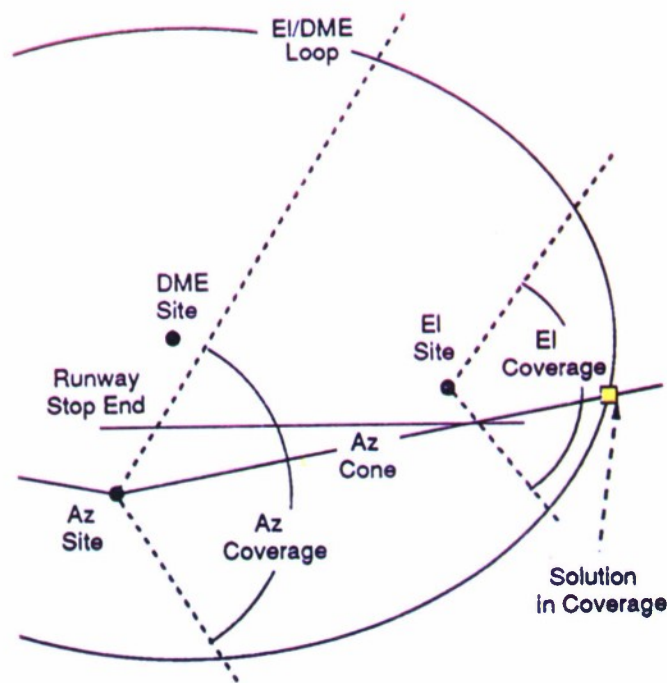


Figure ES-1. A Conventional Siting Geometry for the MLS Ground Units

However, under the present standards of the International Civil Aeronautics Organization (ICAO), designed deliberately to accept a small number of pre existing installations, it is possible to site the ground units in configurations, unconventional according to present understanding and current practice, that have two solutions for aircraft location within the MLS coverage volume. In these situations, in which the DME is distant from the azimuth antenna, the received MLS data do not, and cannot, enable determining in the MLS avionics which is the true solution, and which the false. This is the essence of the multiple solutions problem. Figure ES-2 shows one of the geometries in which multiple solutions in coverage can exist; the two solutions are marked in yellow and blue. The problem of multiple solutions cannot occur with the Mobile MLS, because the azimuth antenna and the DME are collocated.

This problem of multiple solutions appears at present to be unresolved. Exposition, summarized above, and resolution, summarized below, of this problem are the subjects of this report.

Multiple solution geometries can be precluded by the following rule, which can be used either to site the ground units or to define permissible flight paths.

Multiple solutions in coverage cannot occur if, for all possible locations of the aircraft:

- a. For ground operations, or for flight operations using an altimeter, the DME sphere, with center at the DME and radius from the DME to the aircraft, contains the azimuth antenna;
- b. For flight operations involving the elevation antenna, the DME sphere contains both the azimuth and elevation antennas.

Less restrictive, but more complicated, rules for siting the ground units to preclude multiple solutions in coverage are developed in the report.

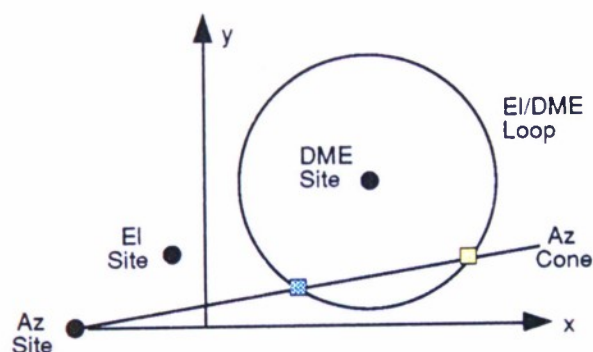


Figure ES-2. An Unconventional Geometry with Two Solutions in Coverage

Examination of the mathematics, geometry, and physics of the MLS shows that up to eight solutions can exist in a completely general configuration of ground units and aircraft; seven of these solutions must be false. This configuration is, fortunately, not operationally possible, but it shows the inherent complexity of the problem. Either two or four real solutions for aircraft position exist in configurations which are possible and are permitted by the present ICAO rules; the other solutions are complex and need not be considered. Although only one real solution can be true, one of the false solutions may lie within the MLS coverage. Position reconstruction algorithms (PRAs) in the MLS avionics convert the signals received from the ground units to aircraft location in Cartesian coordinates; in a multiple solutions situation, those postulated to date can converge to the unique true solution or to a false solution, or can diverge. False solutions outside of coverage, or divergence, can be detected in the avionics and rejected. But if a false solution is within coverage, the MLS avionics is not able to distinguish the true solution from the false using only its own internal data; external data from other sensors are required to select or to find the true solution.

The two principal classes of PRAs – Newton-Raphson and Gauss-Seidel – are examined in the context of multiple solution geometries, and the problems which each type exhibits in the multiple solutions situation are demonstrated.

There are several ways to resolve the multiple solutions problem. The most attractive is to reduce the flexibility of siting of the DME relative to the azimuth antenna so that there can never be more than one solution in coverage, by following the siting criteria noted above. However, this reduces the flexibility of siting of the ground units, or might require additional DME units at some airports. A second means is to design the procedures which specify the approaches that pilots may use in RNAV so that the multiple solutions geometries cannot exist. This might in some situations restrict the flexibility of flight path choice, one of the attractive aspects of the MLS concept; further, if the aircraft is actually in a multiple solutions situation due to an error of pilotage, this could confuse the pilot. However, it may be the best solution for the few airports that now exist with ground unit positioning geometries that permit multiple solutions. A third means is to have the avionics detect unconventional geometries, and advise the pilot thereof. Finally, the avionics could use other instruments and data sources in the aircraft, such as the Global Positioning System or Inertial Navigation System, to enable selection of the true solution within the avionics. This implies significantly more complicated avionics, perhaps involving Kalman filters, or the equivalent, plus the expenses of integration of the other sensors and data sources. This is viewed as the least attractive approach, for such filters in the avionics are complicated, require much storage, and impose large computational burdens, by comparison with the usual PRAs. Further, this approach contradicts the basic MLS philosophy that the data and signals should be so accurate that these sophisticated filters are not required. Finally, it seems counterproductive to modify the design of thousands of avionics units for the sake of a few unconventional ground installations.

It is concluded that the most effective means to deal with the multiple-solutions problem is to preclude it completely by appropriate siting constraints for the DME relative to the azimuth antenna. The best alternate may be to design flight procedures at airports with unconventional geometries such that multiple solution geometries should not occur.



## SECTION 1

### INTRODUCTION

The Microwave Landing System (MLS) may be used both for approach and landing guidance, and also for area navigation (RNAV) operations either in flight or on the ground. These procedures include initial, intermediate, and final approach, landing, steering, deceleration, turnoff, and taxiing. In these functions, the MLS concept uses ground unit siting data, angle signals from an azimuth antenna (Az) and an elevation (El) antenna, and range signals from a Distance Measuring Equipment (DME) transponder, to enable an avionics unit to provide guidance information to the pilot or flight control system. In many of these operations, it is necessary that the avionics use a position reconstruction algorithm (PRA) to determine the aircraft's position in rectangular (Cartesian) coordinates relative to the intended touchdown point on the selected runway. Because of the mathematical complexity of the problem of position reconstruction, PRAs require iterative computational procedures when the three ground units are not collocated.

Examination of the mathematics, geometry, and physics of the MLS shows that up to eight solutions can exist in a completely general configuration of ground units and aircraft; seven of these solutions must be false. This configuration is, fortunately, not operationally possible; it requires a physically impossible location of the DME relative to the other antennas. However, up to four real (plus four complex) solutions for aircraft position exist in configurations which are possible and are permitted by the standards of the International Civil Aeronautics Association (ICAO); only one can be true. Further, one of the false solutions may lie within the coverage of the system in these configurations. PRAs postulated to date for MLS avionics can converge to the unique true solution or to one, or any, of the inherent false solutions. False solutions outside of coverage can be detected and rejected. But if a false solution is within coverage, the avionics cannot distinguish the true solution from the false using only MLS data; external data from other sensors are required to select or to find the true solution. This problem of multiple solutions appears at present to be unresolved. Exposition and resolution of this problem are the subjects of this report.

In normal configurations of the ground unit sites, the azimuth antenna and the DME are collocated at the stop end of the runway, on its extended centerline, and the elevation antenna is near the threshold. In these installations, only one solution is possible within the MLS coverage volume, and there is no problem. However, in order to accommodate a few existing installations, the ICAO rules, in reference 1, permit a wide range of sites for the three ground units. The result is that the current structure of rules permit some unconventional geometries in which multiple solutions for the aircraft location can exist within the MLS coverage. In these geometries, the PRA can find and track a false solution. Moreover, in these cases, the MLS avionics cannot internally detect that there are multiple solutions, nor determine whether the solution to which the iterative process has converged is the true solution, or the false solution within the system coverage volume. The two principal classes of PRAs are known as Newton-Raphson and Gauss-Seidel; both require a priori information that is not available to the MLS avionics in order to select the correct solution in a multiple solutions geometry situation.

Notation is presented in section 2. Section 3 presents the key issue: valid geometries with multiple solutions exist; although these different solutions have different properties, the MLS avionics, as now defined, cannot use these properties to detect and reject a false solution within the system coverage. Sections 4 and 5 show for Newton-Raphson and Gauss-Seidel methods, respectively, the problems which these two classes of algorithms meet in multiple solution situations. Success in resolving the multiple solution problem requires new constraints on the ground equipment siting, or on the flight paths which are allowed for approaching aircraft, thus precluding multiple solutions. Alternately, resolution of this problem can be accomplished by enabling the avionics to detect and reject situations where a multiple solutions geometry can occur, or by use in the MLS avionics of information from other avionics units to enable selecting the unique correct solution. Some suggestions of varying complexity for ground and airborne equipments are offered in section 6. Conclusions follow in section 7. Some of the techniques required to implement the avionics features discussed in section 6 are offered in appendix A, while appendix B examines the question of DME siting constraints which are "sufficient" to preclude multiple solutions in all situations. Each major section of the report terminates with an overview, or summary, of the findings of that section.

## SECTION 2

### COMMON ELEMENTS

Common elements, such as the geometry and the notation, are gathered in this section.

#### 2.1 NOTATION

The coordinate system for the problem is defined in figure 2-1, which shows a completely general configuration of the ground equipments. The x-axis is selected to be the runway centerline and its extension, with positive values towards the approach end and negative values toward the stop end of the runway. The origin of the coordinate system is arbitrarily selected, for the purposes of discussion, to be at the runway threshold, so that normal locations for the ground equipments have negative x-values. Thus, if the azimuth antenna is located near the stop-end of a 5000' runway, its x-value is approximately  $x_A = -5000$ , where the subscript A implies azimuth antenna. The positive direction of y lies to the left of an observer standing at the origin, facing away from the stop end of the runway. The positive direction of z is up, completing the right-hand coordinate system. Upwind and downwind are towards the stop end and towards the threshold, respectively.

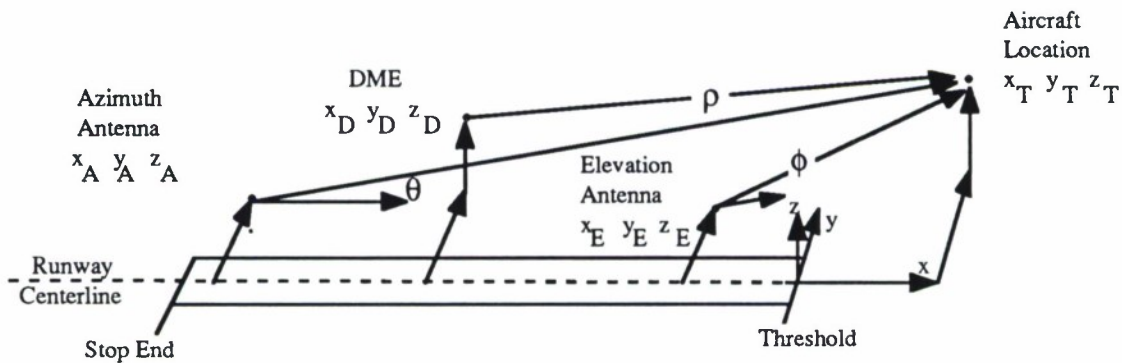


Figure 2-1. Geometry and Notation

The elevation angle is defined as positive counterclockwise, looking along the positive y-axis, so that positive angles correspond to positive altitude when the aircraft is in the coverage of the elevation antenna. Azimuth is defined as positive clockwise from the x-axis, looking down towards the ground, or counterclockwise looking along the positive z-axis. These angle definitions are contrary to the norm for right-handed coordinates, but are consistent with references 1 and 2. It is assumed that the azimuth antenna electronic



boresight is parallel to the runway centerline. This does not imply any loss of generality, for a simple rotation about the z-axis enables a general orientation of the boresight.

The notation is defined.

$x, y, z$	Components of estimated position of aircraft
$x_A, y_A, z_A$	Components of position of azimuth antenna
$x_D, y_D, z_D$	Components of position of DME
$x_E, y_E, z_E$	Components of position of elevation antenna
$x_T, y_T, z_T$	Components of true position of the aircraft
$x_0, y_0, z_0$	Components of the initial position estimate used in the iterative procedures
$\theta$	Azimuth angle at the aircraft relative to the runway centerline, measured at the aircraft in radians (unless otherwise stated)
$\phi$	Elevation angle at the aircraft relative to the horizon, measured at the aircraft in radians (unless otherwise stated)
$\rho$	Slant range of the aircraft from the DME transmitter, measured at the aircraft in feet.

## 2.2 OBSERVATIONS

The observations are defined. The aircraft distance from the DME is

$$\rho = \sqrt{(x_T - x_D)^2 + (y_T - y_D)^2 + (z_T - z_D)^2} \quad (2-1)$$

where the positive value of the radical is required since distance is a magnitude. Notice that a constant distance,  $\rho$ , from the DME defines a sphere with its center located at the DME site. This is true for all geometries, even when the aircraft is not in the volume of coverage of the DME, for example, in the cone of silence directly above the DME. This DME sphere has important properties in defining when multiple solutions occur, their nature, and their avoidance; the term will appear repeatedly.

The azimuth angle observed at the aircraft is

$$\theta = \arctan\{ -(y_T - y_A) / \sqrt{(x_T - x_A)^2 + (z_T - z_A)^2} \}. \quad (2-2)$$



The elevation angle observed at the aircraft is

$$\phi = \arctan\{(z_T - z_E)/\sqrt{(x_T - x_E)^2 + (y_T - y_E)^2}\}. \quad (2-3)$$

The actual observations in (2-2) and (2-3) are the angles which are measured by the avionics; the avionics must deduce the values of the appropriate trigonometrical functions, given the angles. Angles that are observed by the avionics are necessarily within coverage.

In a geometric sense, the azimuth and elevation observation equations, (2-2) and (2-3), define cones. The azimuth cone has its vertex at the azimuth site; the central axis of the azimuth cone is parallel to the y-axis, and the azimuth angle,  $\theta$ , is the external angle between the xz vertical plane and the cone. At any fixed value of y, the radical in (2-2) defines the radius of the cone. Similarly, the vertex of the elevation cone is at the elevation antenna site, the central axis of this cone is parallel to the z-axis, and the elevation angle,  $\phi$ , is the external angle between the horizontal plane and the cone. At any fixed altitude, the radical in (2-3) defines the radius of the elevation cone. Only a portion of these two cones is within coverage.

In (2-1) through (2-3), replace  $x_T$ ,  $y_T$ , and  $z_T$  by x, y, and z, respectively; this replaces the true position of the aircraft, which uniquely defines the observations, by the unknown position, to be determined by the avionics. The mathematical problem of position reconstruction is to solve for the the unknowns, x, y, and z, given the ground unit site data and the observations.

## 2.3 OVERVIEW AND FORECAST

From (2-1)-(2-3), it is seen that every location of the aircraft and ground units forms a set of observations. For every such set, there is a unique value of slant range, from (2-1). Similarly, for every such set of data, there are unique solutions for the azimuth and elevation angles, from (2-2) and (2-3), given the restriction of the arctangent functions to the principal values, in accordance with the usual convention. Therefore, any aircraft location yields a unique set of observations. It will be shown in section 3 that the converse is not true: every set of observations is satisfied by at least two mathematically possible locations of the aircraft. The key concern of this report is that in some allowable geometries there are two possible locations within the MLS coverage volume. In section 3, the geometry of the ground units' sites and the aircraft position will be related to the DME sphere; it will be shown that there can be only one solution in coverage if the DME sphere includes both the azimuth and elevation antennas, but that two solutions in coverage can occur if this criterion is not met.

## SECTION 3

### GEOMETRY AND MULTIPLE SOLUTIONS

In section 2, it was shown that every configuration of the ground unit sites and aircraft location defines a unique set of observations of the range from the DME ( $\rho$ ), the elevation angle ( $\phi$ ) relative to the elevation antenna (El), and the azimuth angle ( $\theta$ ) relative to the azimuth antenna (Az). In this section it will be shown that the converse is not true, and that every set of observations can be mathematically satisfied by at least two locations of the aircraft for any legitimate configuration of the ground units. Not all of these solutions are physically possible, for some are out of coverage. However, in some unconventional geometries of ground unit locations, there can be two solutions for aircraft location within the system coverage volume.

This section presents the concepts of conventional, and unconventional, even abnormal, but legitimate, geometries of ground unit locations, and defines the conditions in which multiple solutions within coverage can occur. According to table A-10 of reference 1, the x-component of position of the azimuth antenna may be anywhere between the elevation antenna's site and 8191 meters (26,834') upwind toward (or perhaps beyond) the stop end of the duty runway; it may not be downwind (forward) from the elevation antenna under any circumstances. However, the DME may be anywhere between 8191 meters upwind to 8191 meters downwind relative to the elevation antenna. Further, the azimuth antenna and the DME may be as much as 511 meters (1676') off the runway centerline, and may even be on opposite sides of the runway from each other.

It is appropriate first to define conventional geometries of ground equipment locations. It will then be possible to show the unconventional geometries, and to contrast their appearance and properties with those of the conventional cases.

#### 3.1 CONVENTIONAL GEOMETRIES

Figure 2-1 showed a typical and conventional layout of the ground units. The azimuth antenna and the DME are near each other, or are collocated, at or near the stop end of the runway, while the elevation antenna is near the threshold.

One very important property of the conventional geometries should be stated at this point. If the DME sphere contains both the azimuth and elevation antennas, then there can be only one solution within coverage for the aircraft location. This property can be used to define the concept of the conventional geometries.

Figure 3-1 expands the idea of figure 2-1 to show the conventional case. As in figure 2-1, the azimuth antenna and the DME are sited near the runway stop end. This arrangement is slightly unconventional only in that the azimuth antenna and the DME are not collocated. The intersection of the mathematical elevation cone with the mathematical DME sphere forms a closed (El/DME) loop, marked as such in the figure. Part of this loop is in coverage, and part is not; but the entire loop is defined. There is only one solution within coverage, at

the extreme right of the diagram, where the azimuth cone, shown in projection, intersects the EI/DME loop. The second solution is at the left edge of the diagram, where the left side of the azimuth cone projection intersects the EI/DME loop. This solution is out of coverage of both the azimuth and elevation antennas, and thus cannot be physically valid; however, it is mathematically valid, since an estimated location of the aircraft at that invalid solution nonetheless satisfies the observed azimuth and elevation angles and the range. That invalid solution can be rejected by the avionics, after it has been found, by reference to the system coverage. The two solutions are color-coded in the diagram; the true solution in coverage is marked as yellow, while the invalid solution is marked red. This color-coding will be used extensively, and consistently, throughout this report.

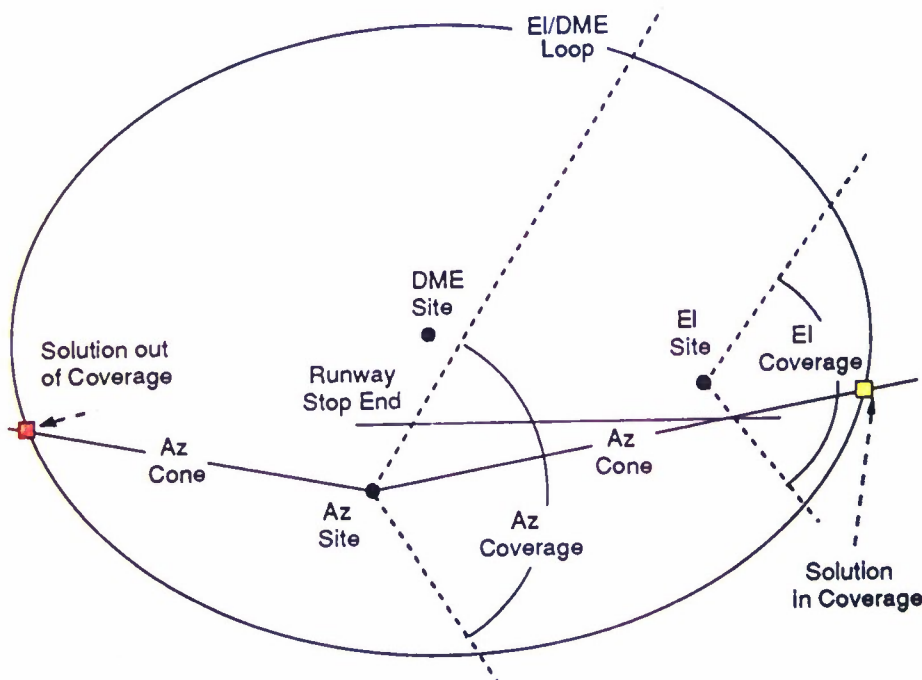


Figure 3-1. A Conventional Siting for the Ground Units

### 3.2 UNCONVENTIONAL GEOMETRIES

Figure 3-2 shows two unconventional geometries, with two solutions in coverage. Although unconventional, these arrangements are not precluded by the constraints of reference 1. They are characterized by the following features:



- a. The DME is located near, or downwind of, the elevation antenna;
- b. The azimuth antenna may be near the stop end of the runway, in a conventional location, or may be, unconventionally, as far downwind as the constraints of reference 1, cited above, allow. In the former, case 1, the two solutions for aircraft location lie in different quadrants of the DME sphere, while in the latter, case 2, the solutions can lie in the same quadrant; this has important implications on the behavior of different types of PRAs;
- c. The DME sphere does not contain both the azimuth and elevation antennas.

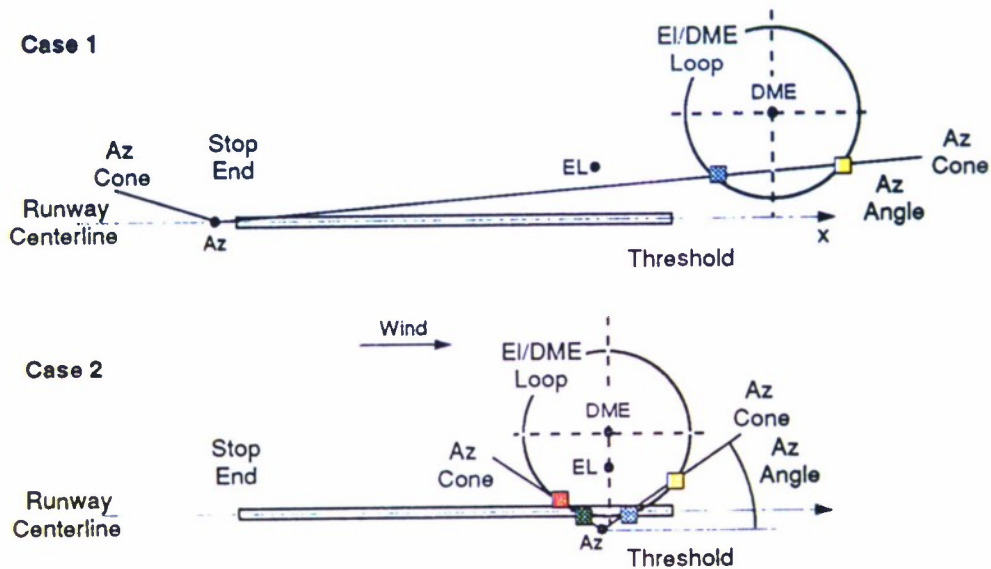


Figure 3-2. Unconventional Sitings for the Ground Units

The geometry of case 1 of this figure could be encountered in a downwind, or in a curved, approach. The geometry of case 2 of this figure could be encountered in a helicopter approach. The solutions are color-coded, with those in coverage marked yellow and blue, and those out of coverage marked in green and red.

Conventional geometries have been defined; in these geometries, both the azimuth and the elevation antennas are within the sphere of distance from the DME to the aircraft. Conversely, in unconventional geometries, one, or both, of the azimuth and elevation antennas is outside the DME sphere, and there are two solutions in coverage that satisfy the observations. The subjects of this study are the behavior of PRAs in unconventional

geometries where two valid solutions within coverage can exist, and the treatment or elimination of this situation.

This section presents the following demonstrations:

- a. There exists a configuration (ground unit and unique aircraft location) for which the set of observations can be mathematically satisfied by eight distinct solutions for aircraft location. This situation is physically impossible, but its existence shows the complexity of the PRA's computational environment;
- b. A variety of physically possible configurations, within the siting constraints of reference 1, exist in which the observation set can be satisfied by four real solutions for the location of the aircraft; two of these locations may lie within the MLS coverage volume;
- c. There are configurations of the ground units which have only two solutions for aircraft location, with both solutions in coverage;
- d. When there are two solutions in coverage, as in (b) and (c), the MLS avionics cannot distinguish the true solution from the false solution without external information to establish which of the two velocity vectors is consistent with the truth. These two solutions imply different velocity vectors, but the MLS has no internal means to detect which is consistent with the truth;
- e. There is, for any siting of the ground units, a unique aircraft flight path such that the two solutions of (d) have identical velocity vectors; this case is defined and is shown to be extremely rare.

These subjects will be treated in order.

It should be understood that the aircraft location must be a set of real numbers, and therefore any complex solution may, and must, be disregarded as extraneous. Thus, a PRA can take advantage of this physical condition and search only for real solutions.

### 3.2.1 Eight Solutions

A geometry which has eight real solutions will be demonstrated, and it will be shown that this is the maximum possible number. This excludes extraneous solutions introduced by mathematical procedures. For example, if (2-2) is squared to eliminate the radical, this doubles the number of possible real solutions; and if (2-3) is also squared, then the number of solutions is again doubled. But the new solutions thus introduced are extraneous, mathematical artifacts to be disregarded or avoided. The algorithms under discussion have specifically been formulated to be free of extraneous solutions.

Assume an elevation angle of ten degrees, for example. Assume the DME transponder is "sited" one mile directly above the elevation antenna; this is obviously physically impossible, and this "site" also violates various constraints of reference 1. Assume that the distance from the DME to the aircraft is slightly less than one mile, so that

the elevation antenna is outside the sphere of loci generated by the DME. Then the elevation antenna's mathematical cone of solution loci intersects the DME mathematical sphere in two circles, one at a lower altitude and the other at a higher altitude. With this assumed

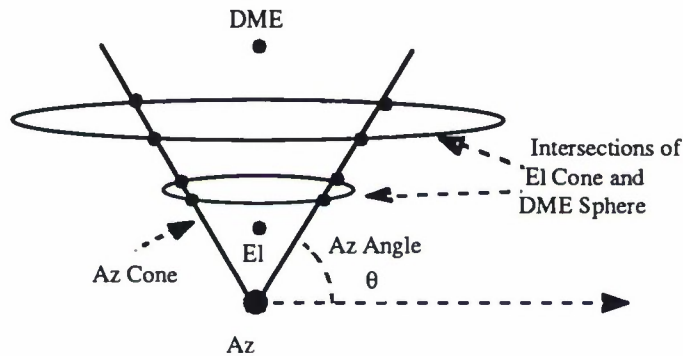


Figure 3-3. Geometry for Eight Solutions

geometry, the two circles are in planes parallel to the ground. The solutions may be on either circle. Now, assume that the azimuth antenna is also outside the DME sphere, perhaps at a normal altitude, and displaced to one side. As shown in figure 3-3, the azimuth cone mathematically intersects each of the two circles at four points, and thus there are eight real solutions. Moreover, study of this geometry shows that eight is the maximum number of real solutions.

Now assume that the DME sphere radius increases without any other change. The diameter of the upper circle in figure 3-3 becomes greater, while the diameter of the lower circle becomes smaller; and when the radius of the DME sphere equals the distance from the DME to the elevation antenna, the lower circle degenerates to a point at the DME, and the four real solutions on that circle degenerate to one repeated solution. Finally, when the radius of the DME sphere exceeds the distance from the DME to the elevation antenna, so that the elevation antenna is within the sphere, then the lower circle vanishes and its four solutions become complex. This is a specific example of a general property of the geometry of the MLS concept: if the vertex of one of the two cones is inside the sphere, there can be no more than four real solutions with one or two in coverage, and if both vertices are inside the sphere, there can be no more than two real solutions with only one in coverage.

It was assumed that the DME site in this example is directly above the elevation antenna site. This is not a rigid requirement for a geometry with eight solutions, and some



horizontal displacement between these units can be allowed without losing any of the solutions. Similarly, some displacement of the azimuth antenna site is also possible. But it must be understood that the entire configuration is physically impossible.

### 3.2.2 Four Solutions

There exists a variety of configurations for which there are four real solutions for aircraft location, with two solutions in the MLS coverage volume. These configurations are physically possible, and are not known to violate any of the various types of siting constraints of reference 1. Further, these configurations, together with those in section 3.3, below, form the set of realizable configurations with two solutions in coverage, the central concern of this study.

Assume that the DME is collocated with the elevation antenna, as suggested in reference 3, and that the azimuth antenna is sited, symmetrically, on the opposite side of the runway. Then,  $x_D = x_E = x_A$ , and  $y_D = y_E = -y_A$ ; this is an unconventional configuration of the ground units, but it is not excluded by reference 1. Note that  $x_A > x_E$  is not allowed by reference 1, while  $x_A = x_E$  is permitted. For simplicity, but without any loss of generality, assume that the ground units are at the ground altitude, so that  $z_E = z_D = z_A = 0$ . The elevation cone intersects the DME sphere in a circle. If the vertex of the azimuth cone is outside the DME sphere, then the azimuth cone intersects this circle at four points. Two of these points may lie within the system coverage. This case is illustrated in figure 3-4,

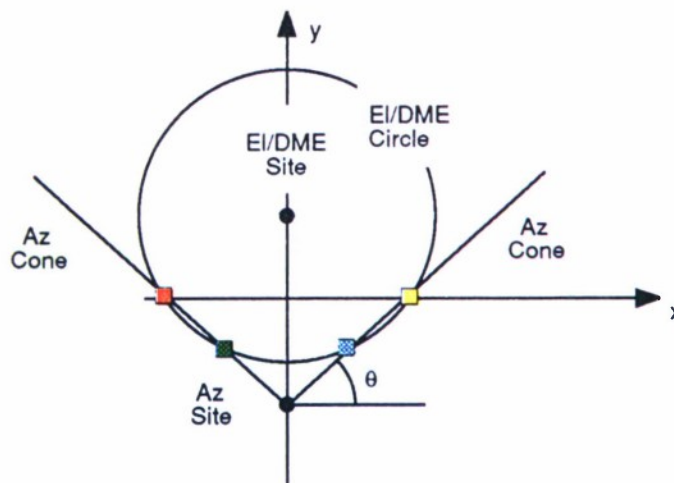


Figure 3-4. Geometry for Four Solutions with Two in Coverage



similar to case 2 of figure 3-2. An equivalent situation exists if the elevation antenna changes its location, so that it is collocated with the azimuth antenna, and the DME is on the other side of the runway. And equivalent geometries are possible if the elevation antenna is anywhere on the line between the azimuth and DME sites, so that  $y_A \leq y_E \leq y_D$ .

Similar to the remarks in subsection 3.1, the ground unit sites have a degree of flexibility which still permits two real solutions within the system coverage. The exact symmetry used in the discussion, above, is not essential.

### 3.2.3 Two Solutions with Both in Coverage

There is another geometry which has two solutions both of which are in coverage, a situation similar to case 1 of figure 3-2. This case is more likely to be encountered, in procedures such as back azimuth operation, or, more generally, in any situation where the DME is downwind from the azimuth antenna. Recall that table A-10 of reference 1 allows the DME to be 8192 meters downwind from the MLS datum point, which is defined as "The point on the runway centerline closest to the phase center of the approach elevation antenna." The geometry which results is shown in figure 3-5. In this figure, the DME is sited downwind relative to the elevation antenna, even further from the runway stop end. The intersection of the elevation cone with the DME sphere forms a closed loop, rather than a circle, and if the elevation antenna site is outside the DME sphere there can be two solutions within the coverage volume of the system.

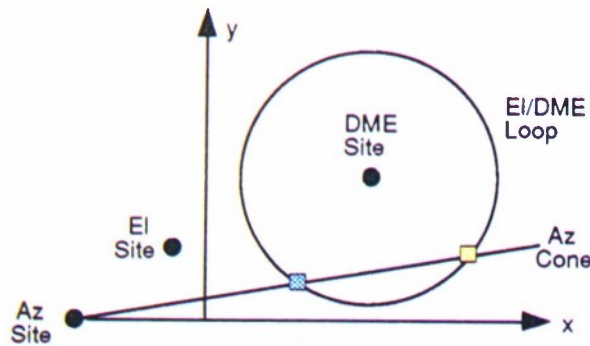


Figure 3-5. Geometry for Two Solutions with Two in Coverage

### 3.2.4 Velocity Vectors

In general, a sequence of observations over time yields a sequence of position estimates. And from this sequence of position estimates it is possible to form an estimate of the velocity vector. If the geometry has multiple solutions in coverage, each of the possible

solution sequences implies a unique velocity vector, as shown in figure 3-6. In this figure, the solid lines represent the situation at  $t = 0$ , while the dotted lines represent the situation one second later. The differences between the solutions for each sequence are the velocity vectors. However, the PRAs in the present generation of MLS avionics have no internal means to tell which velocity vector is true and which is false; this distinction requires integration with other avionic units or, at the risk of confusion, with the pilot, who is in fact an integrating element of the overall air navigation system.

### 3.2.5 Unique Exception

In figure 3-6 it was shown that the velocity vectors which correspond to different aircraft location solutions are distinct and different. It is shown here that there is a unique exception. Assume that the closed loop formed by the intersection of the elevation cone and the DME sphere is tangent to the azimuth cone. Further, assume that the aircraft flight path is such as to maintain this tangency. These two constraints very sharply restrict the possible flight paths. Assume that the aircraft is at zero elevation angle; it is easily shown that the tangency condition requires that the aircraft fly on a circle, shown as a dashed line in figure 3-7, of which the diameter is the Az-DME line. In this figure the solid-line circles represent

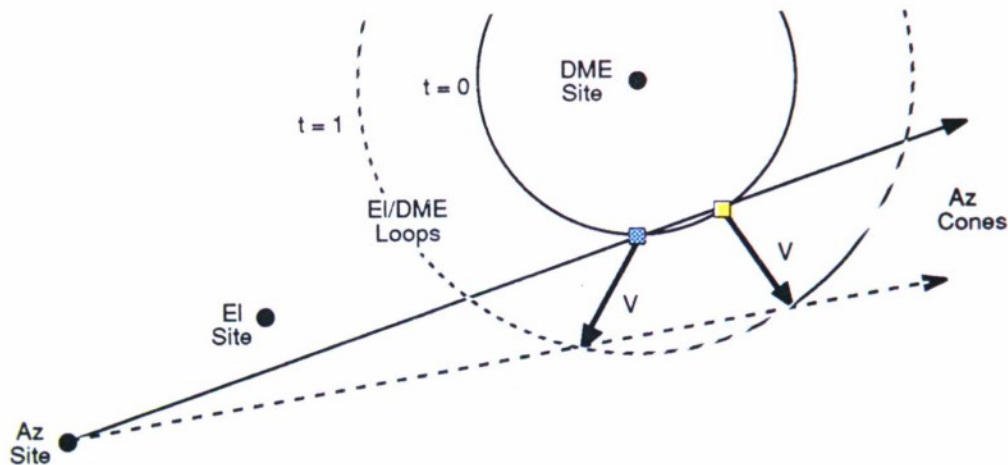


Figure 3-6. Velocity Vectors for Multiple Solutions

the DME sphere at successive instants, while one solid line shows the azimuth cone and line-of-sight at one instant. If the aircraft is at non-zero, or a varying, elevation, then the tangency trajectory becomes more complicated. However, it always remains a unique line in space. Flight on such a path for more than a very few seconds must be viewed as an event of vanishing probability; this case therefore can be neglected.

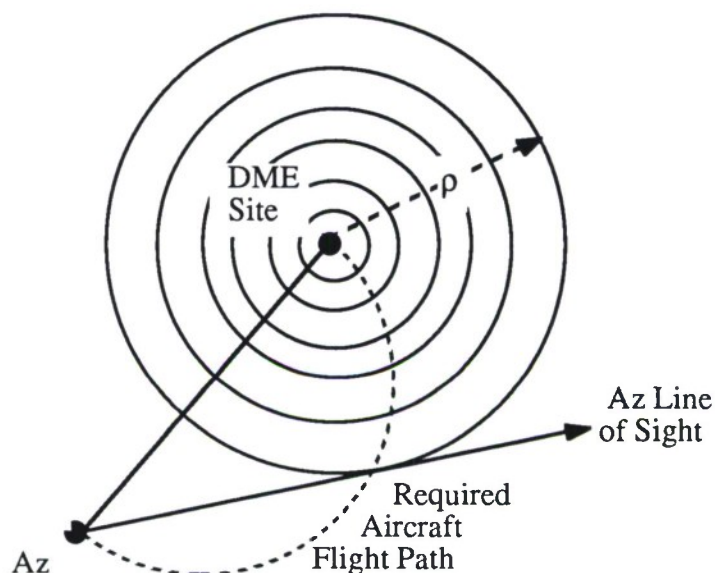


Figure 3-7. Tangency Trajectory

### 3.3 RNAV WITHOUT ELEVATION DATA

According to reference 2, RNAV can be conducted in the regions in which azimuth coverage exists, but outside of elevation coverage. This requires either using altimeter data or assuming that the altitude is zero. Category III (Cat III) operation on the ground comes into this latter class. The same definitions of conventional and unconventional geometries developed above are valid here also. For a conventional geometry of the azimuth antenna and the DME, there is no range sphere for which the aircraft is in the azimuth antenna coverage region but that antenna is outside the sphere. Of course, in these circumstances, the intersection of the range sphere and the constant altitude is a circle parallel to the ground.

### 3.4 OVERVIEW AND FORECAST

In a philosophical sense, the problem of multiple solutions in coverage is that the avionics must know, a priori, which solution is correct. But it is precisely this information which cannot be provided by the MLS avionics. The next two sections examine the specific

and detailed problems encountered by the two classes of PRAs, Newton-Raphson and Gauss-Seidel, which have been examined previously for the MLS application. In the subsequent section, two approaches will be presented for resolution of the multiple solution problem; one approach precludes the problem, while the other solves it.

## SECTION 4

### NEWTON-RAPHSON ALGORITHM

This section shows the behavior of a Newton-Raphson (NR) PRA in the unconventional geometries, discussed in section 3, for which multiple solutions within coverage are possible. The following topics are considered:

- a. The principles of NR iteration are demonstrated and an MLS NR PRA is developed;
- b. The errors of initialization algorithms and observations are demonstrated in a simple geometry with multiple solutions;
- c. The effects of initialization errors are demonstrated: the PRA can converge to false solutions in and even out of coverage.

#### 4.1 A NEWTON-RAPHSON ALGORITHM

The Newton method for solution of higher order functions is demonstrated for a function of one variable; this is then generalized to multi-variable functions to yield an MLS NR PRA, reported previously in references 4, 5, and 6 and repeated here for convenience.

Figure 4-1 shows the region of the continuous function  $y = f(x)$  near a solution. As shown in this figure, Newton iteration assumes a first estimate,  $x_0$ , and calculates the next estimate,  $x_1$ , for the solution of the function by projecting to the x-axis the tangent to the function at  $f(x_0)$ . This is generalized and formally expressed as

$$x_{i+1} = x_i - (f'_i)^{-1}y_i = x_i - (y'_i)^{-1}y_i \quad (4-1)$$

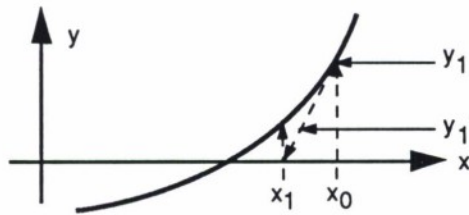


Figure 4-1. Newton-Raphson Iteration in a Single Variable



where  $f'_i$  is the derivative, the slope or gradient, of the function  $f(x)$  with respect to  $x$ , evaluated at the tangency at  $y(x)$ , where  $x = x_i$ . When the derivative is zero, the inversion required by (4-1) cannot be performed; geometrically, it suggests that the next estimate would be at positively, or negatively, infinite values of  $x$ . When this procedure is generalized to multiple variables and expressed in vector/matrix form, it is known as the Newton-Raphson method. The derivative,  $f'$ , is replaced by a matrix,  $J$ , which represents the slope (the gradient) of the multidimensional function at the tangency. This procedure is now shown for the MLS PRA.

From (2-1) through (2-3) respectively, form the error vector  $\underline{f}$ , with components:

from the DME range observation equation

$$f_1 = \sqrt{(x - x_D)^2 + (y - y_D)^2 + (z - z_D)^2} - \rho^2 \quad (4-2)$$

from the azimuth observation equation

$$f_2 = y - y_A + \sqrt{(x - x_A)^2 + (z - z_A)^2} \tan \theta \quad (4-3)$$

from the elevation observation equation

$$f_3 = z - z_E - \sqrt{(x - x_E)^2 + (y - y_E)^2} \tan \phi \quad (4-4)$$

The vector  $\underline{f}$  is zero at the solution,  $f_1 = f_2 = f_3 = 0$ .

The next step in formation of this algorithm is to define the Jacobean matrix, which is the matrix of partial derivatives of the error functions  $f_1$ ,  $f_2$ , and  $f_3$  with respect to the independent variables of aircraft location estimate,  $x$ ,  $y$ , and  $z$ . This matrix is \

$$J = \partial(f_1, f_2, f_3)/\partial(x, y, z) = \begin{bmatrix} (x - x_D) & (y - y_D) & (z - z_D) \\ (x - x_A)\tan\theta/R_A & 1 & (z - z_A)\tan\theta/R_A \\ -(x - x_E)\tan\phi/R_E & -(y - y_E)\tan\phi/R_E & 1 \end{bmatrix} \quad (4-5)$$

where

$$R_A = \sqrt{(x - x_A)^2 + (z - z_A)^2} \quad (4-6)$$

and

$$R_E = \sqrt{(x - x_E)^2 + (y - y_E)^2} \quad (4-7)$$

Iterative algorithms require initial conditions. Given these initial values  $x$ ,  $y$ , and  $z$ , the next, and subsequent, values for the NR PRA are found, analogous to (4-1), according to the rule

$$(x, y, z)_{i+1} = (x, y, z)_i - (J_i)^{-1}(f_1, f_2, f_3)_i \quad (4-8)$$

Like all iterative algorithms, this PRA requires initialization: selecting the first set of position estimates  $x_0$ ,  $y_0$ , and  $z_0$ . The errors of this selection in the context of multiple solutions in coverage will be demonstrated in the next subsection.

The iterative algorithm in (4-7) requires inverting the matrix  $J$ , evaluated at the iteration  $i$ . But when the determinant of this matrix is null, with value of zero, the inversion process cannot be performed. This is a true analogy with the single-variable process outlined earlier, for it indicates that the gradient of the multivariable function is zero. This situation is known as a singularity of the matrix. There is a singularity between every pair of solutions. Singularities are the source of the problems which NR PRAs exhibit in the MLS multiple solution case, and are thus examined further.

Assume that the three ground units are on a straight line, so that  $x_D = x_A = x_E$ , as in figure 3-4 and case 2 of figure 3-2 in the previous section. Further, assume that the three ground units are at the same height, zero, so that  $z_D = z_A = z_E = 0$ . These latter assumptions are close enough to being true to be meaningful, and at the same time result in valuable simplifications of the algebra.

Under these assumptions, set  $f_3 = 0$  and solve for  $z$ . Then substitute the result into (4-2) and (4-3); this step leaves two quadratic equations, in  $x$  and  $y$ . Now set  $f_2 = 0$  in (4-3) and solve for  $y$ ; this reduces the problem to a projection along the azimuth antenna line of sight to the aircraft. Then substitute this result into (4-2). Squaring then yields a quartic in  $x$  alone. This quartic,  $q(x)$ , must have either two or four real solutions, and must have a horizontal tangency – a singularity – between each pair of solutions. The left side of figure 4-2 shows the form of this quartic. In this figure, the four solutions are color coded; the yellow and blue solutions are within coverage, and the green and red solutions are out of coverage. The singularities are marked L (left), C (central), and R (right).

The singularities may also be found directly from (4-5), whence the determinant of the square matrix  $J$  is

$$\Delta = |J| = (x - x_D)[1 - (y - y_D)\tan\theta/R_A](1 + z\tan\phi/R_E) \quad (4-9)$$

The singularities are found when  $\Delta = 0$ . They may be shown in the  $xy$ -plane as trajectories, enabling comparison with the equivalent quadratic equation on the left of this figure.

The first term of (4-9) yields

$$x_S = x_D \quad (4-10)$$

where the subscript  $S$  denotes singularity. This is a central singularity; it is labelled  $C$  in the right side of figure 4-2 and corresponds to the singularity  $C$  on the left of the diagram. A vertical plane, parallel to the  $yz$ -plane, it passes through the line joining the three ground



units. This singularity separates the inboard pair of solutions, coded in green and blue in the figure.

The second term of (4-9) is

$$yS = yD + \sqrt{(x - x_A)^2 + z^2} \tan(90 - \theta) \quad (4-11)$$

This is a cone, with its central axis of radial symmetry parallel to the y-axis. The vertex is at  $x = x_A$ ,  $y = y_D$ , and  $z = 0$ , and its central interior angle is  $\theta$ ; see the discussion in the paragraphs below (2-3) for the important distinctions between the internal and external angles of the cones. If the observation cone is concave in the positive-y direction, this singularity cone is concave in the negative-y direction. At any constant altitude, the intersection of this cone with a horizontal plane is a hyperbola. Labelled LR in the figure, this hyperbola separates the inner from the outer for aircraft location. The color-coding and LCR notation are consistent with the left of figure 4-2.

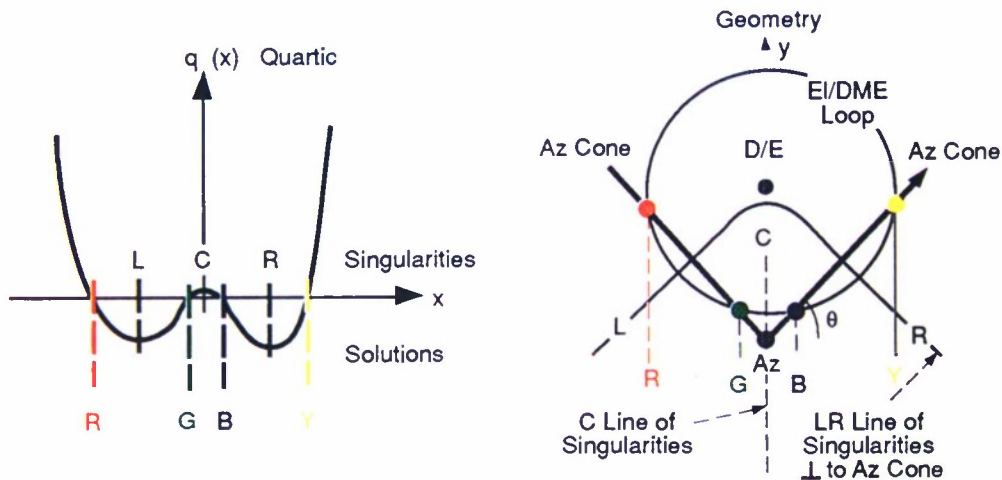


Figure 4-2. Locations of Solutions and Singularities in the Symmetric NR PRA Problem

The third term of (4-9) yields

$$zS = -\sqrt{(x - x_E)^2 + (y - y_E)^2} \tan(90 - \phi) \quad (4-12)$$

This also is a cone, with central axis of radial symmetry parallel to the z-axis. The vertex is at  $z = 0$ , the cone is concave down, and its central internal angle is  $\phi$ ; see, again the discussion below (2-3). This cone of singularities is always at negative altitude, and thus is always out of coverage.

If the estimated location at any iteration is near a singularity, the next estimate will be far distant. This next estimate may converge to a true solution, or may converge to a false

solution, perhaps out of coverage. It is even possible for the solution to diverge, a very rare occurrence in NR algorithms.

If the location of the DME is moved to the right, so that the situation becomes similar to figure 3-5, or to case 1 of figure 3-2, then the quartic becomes unsymmetric, as shown in the left of figure 4-3; the yellow and blue solutions remain, while the green and red solutions become complex and of no interest. But as there are two solutions, there is a singularity  $R$  between them. To the right of the singularity, any initialization converges towards the yellow solution, and the yellow well of attraction is the semi-infinite half-plane. Some, but not all, initializations to the left of the singularity  $R$  are in the well of attraction of the blue solution. Thus, any initialization in either of the two narrow, yellow, regions on the left of this singularity leads to the yellow solution. As before, the yellow and blue solutions are on the downwind side of the azimuth cone where true solutions can exist in coverage. As stated above, the green and red solutions are complex.

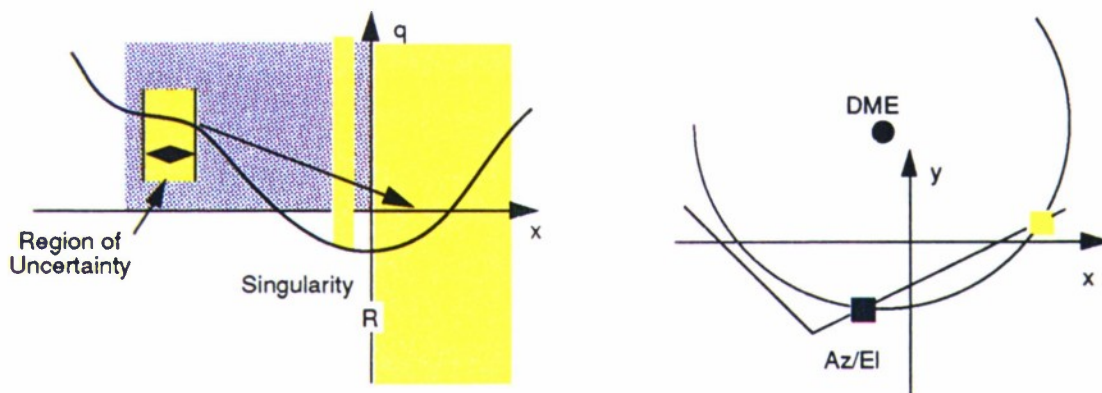


Figure 4-3. Solutions and Singularities in an Unsymmetric Geometry

## 4.2 ERRORS IN INITIAL CONDITIONS

Like all iterative procedures, NR algorithms require an initial condition at which to start the search for a solution. When a problem has only one real solution, any initial condition that does not lead to divergence will converge to that solution, but when there are two or more solutions, then the choice of the initial condition determines the solution to which the process converges. The accuracy of various initializing procedures and algorithms is now considered.

### 4.2.1 Initializing Algorithms

A number of different initializing algorithms have been proposed in references 2, 4, 5, and 6. The best of these will be evaluated in a geometry similar to figure 3-2, where the DME and elevation antennas are assumed collocated while the azimuth antenna is symmetrically located across the runway. The several initializing algorithms are defined.

Type 1

$$\begin{aligned}x_0 &= (x_D + \rho)\cos\theta\cos\phi \\ y_0 &= y_A - (x_D - x_A + \rho)\sin\theta\cos\phi \\ z_0 &= z_E + (x_D - x_E + \rho)\sin\phi\end{aligned}$$

Type 2

$$\begin{aligned}x_0 &= x_D + \rho\cos\{\theta + \sin^{-1}[(x_D - x_A)\sin\theta/\rho]\} \\ y_0 &= y_A - \rho\sin\{\theta + \sin^{-1}[(x_D - x_A)\sin\theta/\rho]\} \\ z_0 &= z_E + \rho\sin\{\phi + \sin^{-1}[(x_D - x_A)\sin\theta/\rho]\}\end{aligned}$$

Type 3

$$\begin{aligned}x_0 &= x_D + \rho\cos\theta\cos\phi \\ y_0 &= y_A - \rho\sin\theta\cos\phi \\ z_0 &= z_E + \rho\sin\phi\end{aligned}$$

Assume  $x_D = x_A = x_E = 0$ ,  $y_D = -y_A = -y_E$ , and  $z_D = z_A = z_E = \phi = 0$ , then the three become identical, yielding

$$\begin{aligned}x_0 &= \rho\cos\theta \\ y_0 &= y_A - \rho\sin\theta \\ z_0 &= \rho\sin\phi\end{aligned}\tag{4-13}$$

These assumptions are consistent with the geometry of figure 3-4.

Table 4-1 shows the assumed locations of the ground equipments, the locations for the aircraft consistent with the observations, and the initializations estimated by the initialization algorithms.

**Table 4-1. Performance of Initialization Algorithms**

Aircraft Locations		Initialization Algorithm	
	Blue	Yellow	Estimates
x0	394.90	2203.20	2424.87
y0	-1272.00	-228.00	-100.00
z0	0.00	0.00	0.00

Observations:  $\rho = 2800.00$ ,  $\theta = -30.00^\circ$ ,  $\phi = 0.00^\circ$

Ground Unit Sites			
	DME	Azimuth Antenna	Elevation Antennna
x	0	0	0
y	1500	-1500	1500
z	0	0	0

---

Even in this very ideal situation, the errors of initialization are of the order of 220' for the yellow (downwind) solution, and of the order of 2000' for the blue (upwind) solution. These algorithms are designed for the yellow (downwind) solution rather than the blue, but without a priori knowledge of which solution is desired it is not possible to do better.

#### 4.2.2 Observation Errors

The errors in the observations also contribute to errors in the initialization. From (4-13), the error terms are

$$\begin{aligned}\Delta x &= \Delta \rho \cos \theta - \rho (\Delta \theta) \sin \theta \\ \Delta y &= -\Delta \rho \sin \theta - \rho (\Delta \theta) \cos \theta\end{aligned}\tag{4-14}$$

The second term in these error expressions is due to azimuth angle errors, and is negligible. But with a TACAN-type DME, the error in the range observation may be of the order of 0.1 nautical mile, or 628', so that the error contributions become  $\Delta x = 544'$  and  $\Delta y = 314'$  in the case under study.

Notice the geometry in figures 3-4 and 3-5 in the context of range observation error. If the geometry is such that the azimuth line of sight is almost tangential to the DME sphere, then a negative error of range can result in a computational situation in which there is no real solution whatever. This possibility affects both the NR, and the Gaussian types of PRA to be discussed in the next section. Means of dealing with this error will be discussed in section 6.



### 4.3 THE EFFECTS OF INITIALIZATION ERRORS

There are two distinct problems in NR PRAs in the MLS context. The first is that when there are two solutions in coverage, there is no way for the algorithm internally to select the correct initialization and thus the correct solution. The second problem is that the combination of DME observation errors and initialization algorithm errors can cause the NR PRA to converge to a false solution. Discussion of solutions to the first problem is deferred to a later point in this report, while the consequences of imperfect initialization are demonstrated hereunder.

Consider figure 4-4, an expansion of the left side of figure 4-2. It shows the quartic function which can be written for this geometry. An initialization in the yellow region, which has a left boundary on the singularity, R, converges to the solution marked Y, in that space. The same is true for the symmetrical red region and its boundary, L, on the left of the figure. But, near the central singularity, C, lies a pair of "wells of attraction," colored green and blue, within which are the green and blue solutions. An initialization in either of these wells converges to the solution within that well. The boundaries of the wells are defined by the requirement that the increment  $(-J^{-1}\hat{f})$  at the left edge of a well be equal in magnitude and opposite in sign to the increment at the right edge of the well. These boundaries form a limit cycle. Since the geometry has an assumed right-left symmetry, there is also a figure-8-shaped limit cycle which is also shown in the diagram. It is difficult in the extreme to forecast the ultimate solution to which an initialization that is not in one of the four wells of attraction will converge. It might be guessed that initializing just to the left of the singularity R might converge to the red solution, and that initializing just to the right of the central singularity C might converge to the yellow solution, but these are no more than guesses.

Figure 4-5 shows the solution to which the NR PRA converges as a function of the  $x_0$  and  $y_0$  initial conditions, under the assumption that  $z_0 = z_T$ . In this figure, the DME and the elevation antennas are assumed to be collocated at the elevation antenna site, marked at the top of the figure by a black triangle. The azimuth antenna is at the black triangle near the bottom of the figure. The red, green, blue, and yellow solutions are white diamonds in the red, green, blue, and yellow fields, respectively. An initial condition of  $x_0$  and  $y_0$  is at the center of each 100' by 100' square. The blank column at the center of the diagram is the central singularity C, at  $x = x_D$ . The LR singularity lies at the boundary between the red and the blank regions on the left, and between the yellow and blank regions on the right. The blank regions near the LR

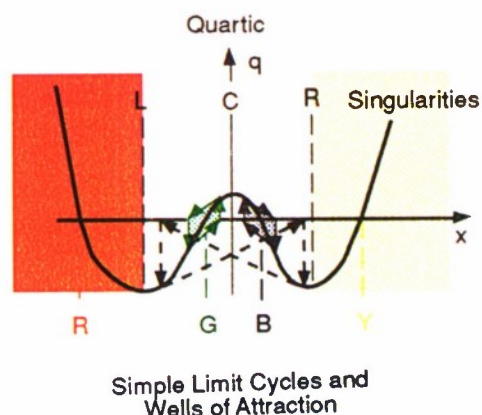


Figure 4-4. Simple Limit Cycles and Wells of Attraction

singularity are initializations whence the NR PRA actually diverges without limit; the estimates oscillate between a blank location on the right to a blank region on the left, then back to the right, and so on, with the y-component becoming more negative at each iteration.

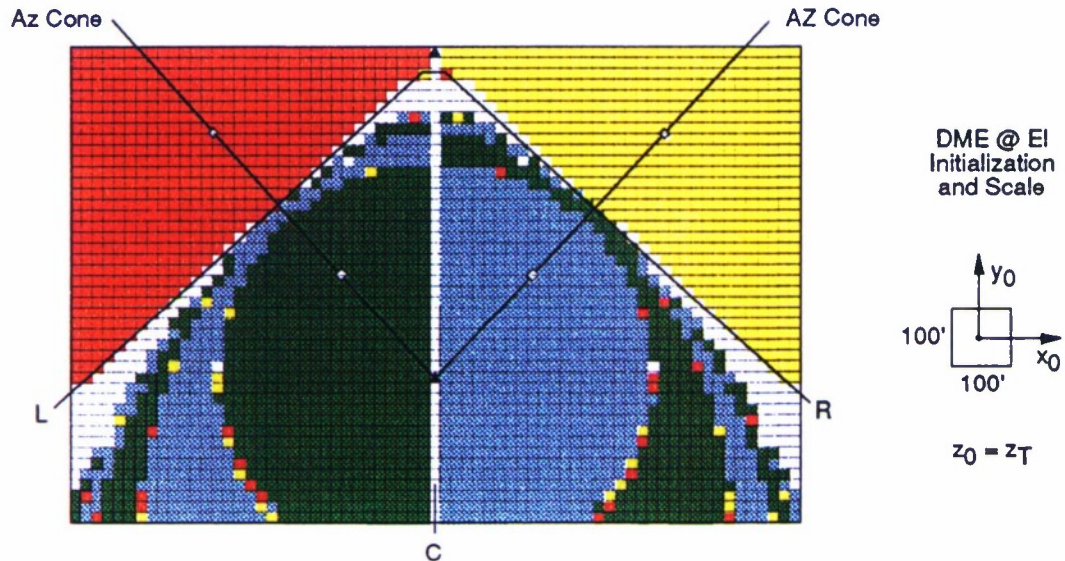


Figure 4-5. Initializations and Solutions: Symmetrical Case

The line of sight, along the surface of the azimuth cone, from the blue solution to the yellow passes out of the blue well of attraction at about 600' from the blue solution, and crosses the singularity R about 200' farther out, and the singularity R is about 700' from the yellow solution. The results in 4.2.2 show that errors of  $\Delta x = 544'$  and  $\Delta y = 314'$  can easily occur; these are sufficient to place the initial estimate in the interface between the blue well of attraction and the yellow infinite half-plane.

The blue-yellow interface region in figure 4-5 is expanded to a scale with 10' by 10' squares in figure 4-6. This figure shows that every solution exists within this small region; even blank squares implying divergence can be found. The blue and yellow solutions are in coverage, while the other two are out of coverage.

The situation changes only slightly if the elevation and azimuth antennas are collocated, with the DME on the other side of the runway. The only significant change is that divergence no longer appears; the blank spaces in figure 4-6 near the R singularity now converge to the red solution, which is out of coverage, while the blanks near the L singularity converge to yellow. See figure 4-7, where the solutions in coverage are 400' apart, so that the azimuth line of sight is more nearly tangent to the DME sphere. This figure is interesting and somewhat deceptive, for it suggests that the confusion and ambiguity at the boundary between the blue and yellow solutions has vanished due to the proximity of the solutions.



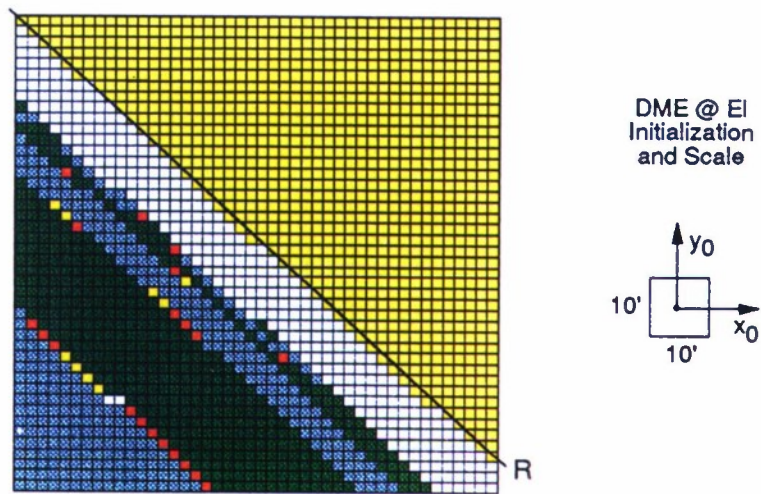


Figure 4-6. The Blue-Yellow Interface, Expanded

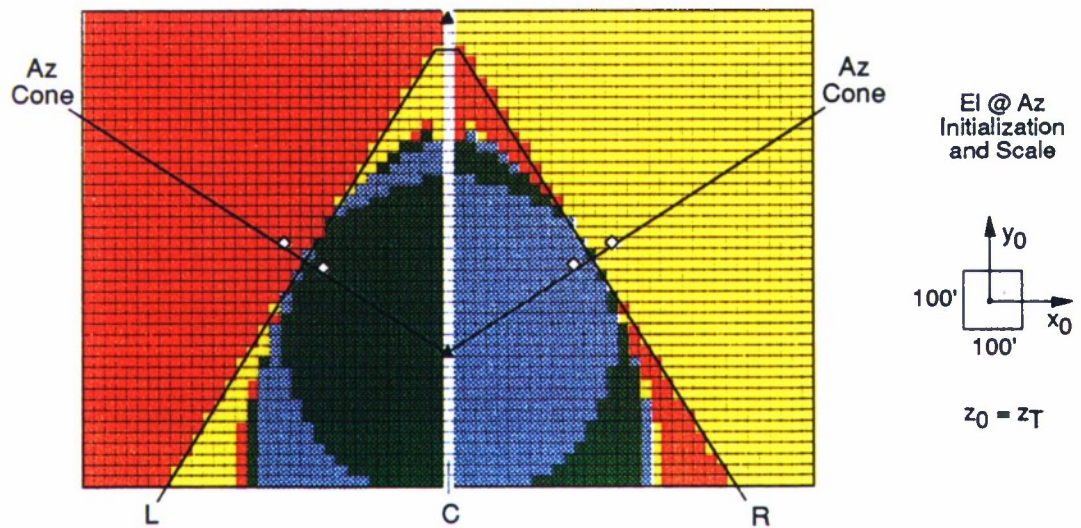


Figure 4-7. Initializations and Solutions: Near-Tangency Case

Figure 4-8 expands the scale of figure 4-7 by a factor of 100; each square now represents 1'. In this figure the boundary between the blue and yellow wells of attraction



appears as a richly confused, chaotic, area which shows that every one of the four solutions may actually be reached. This is to be expected, since, as remarked above, there is at least one singularity between every pair of solutions, and initializations near a singularity can easily lead to the wrong solution.

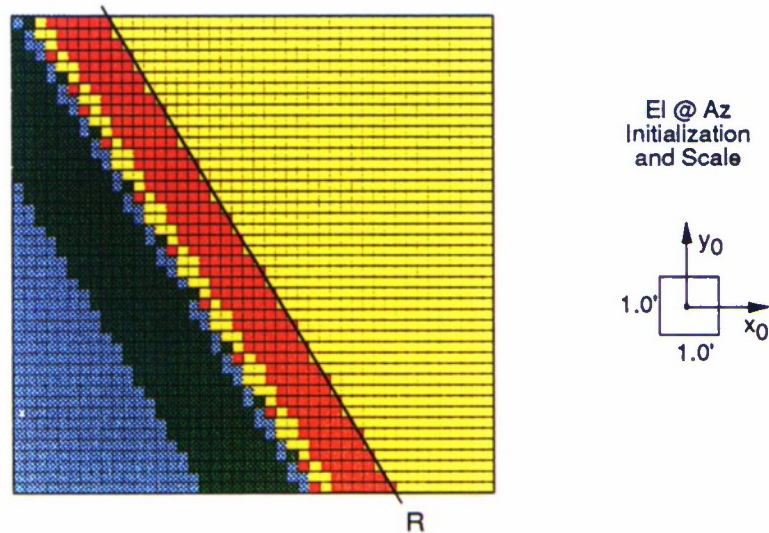


Figure 4-8. The Blue-Yellow Interface in Near-Tangency Case

Assume that the DME is sited downwind from the other two units, which, for simplicity, are assumed to be across the runway from each other. This results in an unsymmetric geometry which is similar to figure 4-3. The quartic equation becomes unsymmetric as shown in the left of figure 4-9, and the red and green solutions become

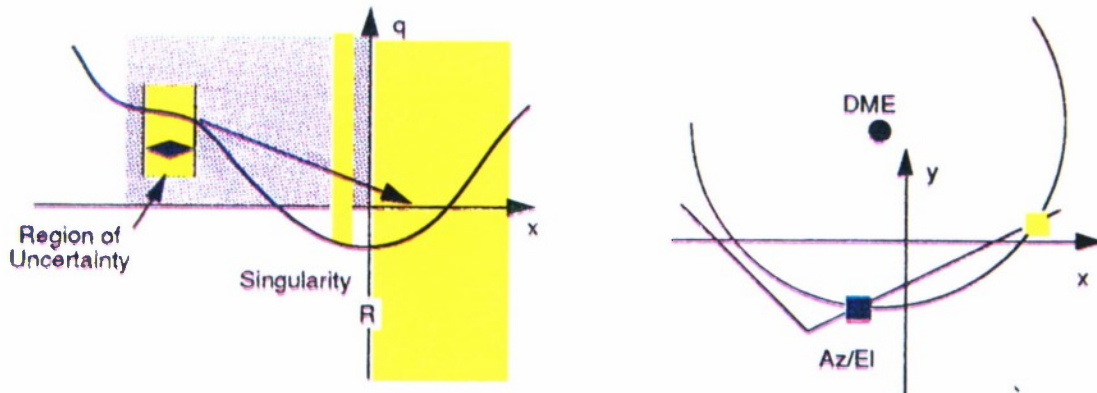


Figure 4-9. Small Downwind Displacement of DME

complex and inaccessible. The right of this figure shows the geometry, the sites of the several units, and the form of the azimuth cone and the EI/DME loop intersection. The left side of this figure shows that there are at least two regions, in the left part of the diagram, where an initialization that should presumably lead to the blue solution actually leads to the yellow solution. The effect of the absent red and green solutions, now complex, is still felt.

This is confirmed in figure 4-10, where the DME is located 2000' downwind from the other two units. The region between the R-singularity and the blue well of attraction, whose outline can be recognized, still enables converging to the wrong solution. With larger downwind displacement of the DME, the false solution problem ultimately vanishes.

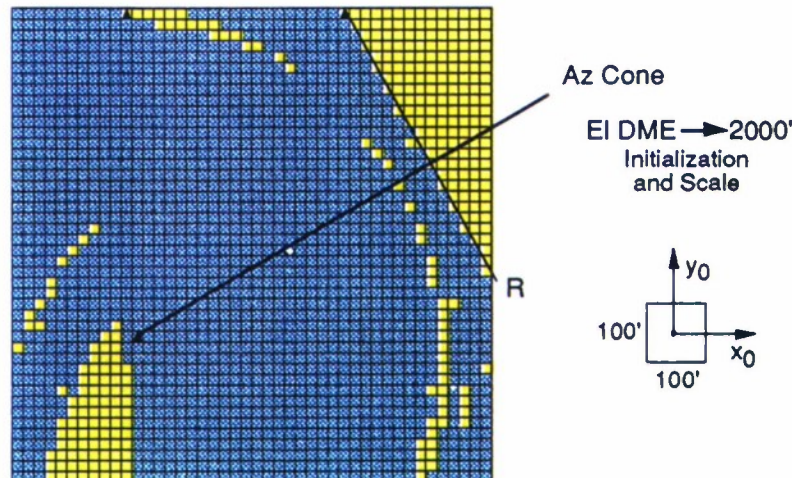


Figure 4-10. Effect of Large Downwind Displacement of DME

#### 4.4 OVERVIEW OF NR ALGORITHM RESULTS

In the unconventional geometries with which this report is concerned, an NR PRA can converge to false solutions, even to false solutions out of coverage, due to errors in the observations and the initializations. When the DME is sited towards the threshold relative to the other antennas, so that there are only two solutions with both in coverage, an initialization in the general area of the well of attraction for the upwind (blue) solution can inadvertently



converge to the yellow solution. However, an initialization in the yellow solution's well of attraction, a semi-infinite half-plane, will always converge to the yellow solution.

The results presented above follow from one particular means for NR solution of this problem. Others exist, or can be devised; a different NR approach is presented as Case 12 of appendix D of reference 2. However, the NR PRA presented above in this report has the least number of possible real solutions, and thus the least number of the singularities that are the source of the difficulties with this technique for solution of sets of coupled nonlinear equations.



## SECTION 5

### GAUSS-SEIDEL ALGORITHMS

The behavior of Gauss-Seidel (GS) PRAs in the unconventional geometries of this study is now considered. The principles which underly this class of iterative algorithms are outlined, followed by a general discussion of their problems in the MLS PRA context.

#### 5.1 THE GAUSS-SEIDEL PRINCIPLE

The GS method solves each equation for one variable, and evaluates each equation using the newest data at each step. In the MLS case, this yields:

Setting  $f_3 = 0$  in (4-4), the elevation equation yields the rule

$$z_{i+1} = z_E + \sqrt{(x_i - x_E)^2 + (y_i - y_E)^2} \tan \phi \quad (5-1)$$

Setting  $f_2 = 0$  in (4-3), the azimuth equation similarly yields

$$y_{i+1} = y_A - \sqrt{(x_i - x_A)^2 + (z_{i+1} - z_A)^2} \tan \theta \quad (5-2)$$

Finally, setting  $f_1 = 0$  in (4-2), the range equation similarly yields

$$x_{i+1} = x_D - \sqrt{\rho^2 - (y_{i+1} - y_D)^2 - (z_{i+1} - z_D)^2} \quad (5-3)$$

where the positive sign of the radical is used if  $x_0 > x_D$  and the negative sign otherwise.

This conventional approach to developing a GS PRA was used in reference 2. It converges successfully in most, but not all, conventional geometries; see reference 3.

As with the NR PRAs, the GS PRAs have no internal mechanism to enable deciding whether or not  $x_0 > x_D$ , a key issue in (5-3). However, once that decision is made, by whatever means, the GS algorithms which are known, see references 2, 4, 5, and 6, behave in easily-described ways. Two other important points should be made here:

- a. The radicand in (5-3) can be negative in some circumstances, and a negative radicand trap is essential;
- b. The sequence in which the equations are solved sharply influences the stability of GS algorithms; different sequences can be appropriate in different geometries.



The conventional GS PRA is essentially defined by (5-1) through (5-3); two alternatives are very briefly outlined. These are called the Rotational Gauss-Seidel (RGS) and the Successive Partial Relaxation (SPR) GS PRAs; see references 5 and 6. The former operates on this principle: a new coordinate system is defined with origin at the azimuth antenna; it is rotated such that the lateral position estimate  $y^*$  of the aircraft in these translated and rotated coordinates becomes exactly zero. The latter PRA increments the prior estimate by the product of the relaxation factor  $\omega$  and the difference ( $\Delta$ ) between the prior and proposed solutions; the factor  $0 < \omega < 2$  is calculated as a function of the geometry. These two algorithms require initialization of  $x_0$ ,  $y_0$  and  $z_0$ , are slightly less compact than the conventional GS PRA, and have a somewhat greater computational burden. However, for the yellow solution, they are stable and converge rapidly everywhere within the MLS coverage volume.

The behavior of these three GS PRAs in the multiple solution situations is now examined. The dichotomy imposed by the necessity of choosing the appropriate sign of the radical forms a natural basis for classifying and demonstrating the problems encountered by GS algorithms in the vicinity of the blue solution.

## 5.2 SOLUTIONS IN SAME QUADRANT

The geometry in this situation is described by case 2 of figure 5-1. The DME is collocated with the elevation antenna at the elevation antenna site, and the azimuth antenna is sited symmetrically on the opposite side of the runway. The two solutions for aircraft location are presented below, in table 5-1, together with the observation data common to both locations, and the site geometry data.

**Table 5-1. Aircraft and Ground Unit Geometry: One-Quadrant Case 2**

	Aircraft Locations		Ground Unit Sites			Observation Data
	Blue	Yellow	Az	El	DME	
x	900	2092.0	0	0	0	Slant-Range, $\rho = 2286.9'$
y	- 600	581.6	-1500	1500	1500	Azimuth Angle, $\theta = -44.82^\circ$
z	100	100.0	0	0	0	Elevation Angle, $\phi = 2.51^\circ$

The behavior of these three GS PRAs in search for the blue solution is shown in table 5-2. For this table, the algorithms were initialized very near the blue solution, with errors of 10' in the x and y directions to demonstrate their characteristic performance in this geometry.

The table is organized in three groups, one for each algorithm. The top group is for the conventional, the second is for the rotational, and the third is for the successive partial relaxation PRA. In each group, the first column shows the location of the blue solution, and the second column shows the assumed initialization. The next six columns show the output after each iteration.

**Table 5-2. Behavior of Gaussian Algorithms at Blue Solution in One-Quadrant Case**

Conventional GS PRA								
	Blue Loc.	Init.	Estimated Location after Iteration n					
			n = 1	2	3	4	5	6
x	900.00	910.00	922.68	950.58	1008.67	1117.85	1291.70	1512.56
y	-600.00	-590.00	-590.15	-577.59	-550.02	-492.59	-384.55	-212.36
z	100.00	100.00	99.77	100.00	100.00	100.00	100.00	100.00
-----								
Rotational GS PRA								
	Blue Loc.	Init.	Estimated Location after Iteration n					
			n = 1	2	3	4	5	6
x	900.00	910.00	2088.97	2092.02	2092.01	2092.01	2092.01	2092.01
y	-600.00	-590.00	578.57	581.60	581.59	581.59	581.59	581.59
z	100.00	100.00	100.00	99.93	99.93	100.00	99.99	100.00
-----								
Successive Partial Relaxation PRA								
	Blue Loc.	Init.	Estimated Location after Iteration n					
			n = 1	2	3	4	5	6
x	900.00	910.00	922.84	937.09	959.54	993.91	1044.40	1114.59
y	-600.00	-590.00	-590.07	-583.71	-573.47	-557.22	-532.05	-494.41
z	100.00	100.00	99.77	100.00	100.00	100.00	100.00	100.00

Table 5-2 shows that the conventional and SPR algorithms appear to be converging slowly towards the yellow solution, although initialized almost exactly at the blue solution. The rotational PRA converges rapidly to the yellow solution. For all three PRAs, the blue solution is apparently invisible. The SPR PRA can be modified, by an appropriate change of the relaxation factor,  $\omega$ , to converge more rapidly to the yellow solution. All three can be modified, by reconfigurations such as a change in the sequence in which the equations are used, to converge to the blue solution; however, in this case, they will not be able to find the yellow solution.



### 5.3 SOLUTIONS IN TWO QUADRANTS

This situation is described by case 1 of figure 5-1: the azimuth and elevation antennas are assumed to be in the same locations as in case 2, but the DME is assumed to be 2000' downwind. The two solutions are in different quadrants, as shown in that figure. Further, this two-quadrant geometry persists if the azimuth antenna is in its conventional location near the stop end of the runway. In principle, this should be an easier problem for the GS PRAs, for there is only one solution in each quadrant, and the two quadrants are separated by the boundary at  $x = x_D$ , where the negative-radical trap must operate. Table 5-3 shows the locations of the several ground units, analogous to table 5-1; however, as there is only one solution, for which  $x < x_D$ , the other solution is not shown.

**Table 5-3. Aircraft and Ground Unit Geometry: Two-Quadrant Case 1**

	Aircraft Location	Ground Unit Sites			Observation Data
	Blue	Az	El	DME	
x	1525	0	0	2000	Slant-Range, $\rho = 2155.4'$
y	-600	-1500	1500	1500	Azimuth Angle, $\theta = -30.49^\circ$
z	100	0	0	0	Elevation Angle, $\phi = 2.21^\circ$

Table 5-4, following the format of table 5-2, shows the behavior of the three PRAs at the blue solution; the references previously cited adequately show their behavior at the yellow solution for this class of geometries. The conventional algorithm diverges until it enters the negative-radical trap at the fourth iteration; the entry of zeros for all variables has been chosen as the indicator of this event. The rotational algorithm, in the second group, converges as desired to the blue solution. The successive partial relaxation algorithm converges, but slowly and in an oscillatory pattern, towards the blue solution. The initialization was chosen very close to the true blue solution, to enable and invite comparison to table 5-2. With less favorable initialization, better behavior cannot be expected, except by chance. Again, it should be anticipated that the conventional, rotational, and partial relaxation algorithms could yield better performance if reconfigured.

**Table 5-4. Behavior of Gaussian Algorithms at  
Blue Solution in Two-Quadrant Case**

**Conventional GS PRA**

	Blue Loc.	Init.	Estimated Location after Iteration n					
			n = 1	2	3	4	5	6
x	1525.00	1535.00	1499.73	1596.20	1367.92	.00	.00	.00
y	-600.00	-590.00	-594.13	-614.88	-558.08	.00	.00	.00
z	100.00	100.00	99.92	99.25	102.09	.00	.00	.00

**Rotational GS PRA**

	Blue Loc.	Init.	Estimated Location after Iteration n					
			n = 1	2	3	4	5	6
x	1525.00	1535.00	1526.53	1525.00	1525.00	1525.00	1525.00	1525.00
y	-600.00	-590.00	-599.09	-599.99	-600.00	-599.99	-599.99	-599.99
z	100.00	100.00	100.11	100.00	100.00	100.00	100.00	100.00

**Successive Partial Relaxation GS PRA**

	Blue Loc.	Init.	Estimated Location after Iteration n					
			n = 1	2	3	4	5	6
x	1525.00	1535.00	1490.59	1552.06	1507.94	1537.55	1516.67	1530.95
y	-600.00	-590.00	-591.92	-605.99	-596.03	-602.82	-598.08	601.35
z	100.00	100.00	99.92	98.97	100.80	99.49	100.37	99.75

## 5.4 OVERVIEW OF GS ALGORITHM RESULTS

In geometries where the two solutions in coverage are in the same quadrant of the DME-El loop, GS algorithms behave incorrectly near the blue solution, and either diverge or converge to the downwind yellow solution.

In geometries where the two solutions in coverage are in different quadrants of the DME/EL loop, the necessity of preselecting the correct sign of the radical in (5-3) reduces the problem to a situation where there is only one solution. These algorithms have varying measures of success in finding the blue solution; the conventional GS PRA diverges in some cases, while the rotated-coordinates and partial-relaxation PRAs of references 5 and 6 are stable and converge to the blue solution.

When the two solutions are in different quadrants, it is important to appreciate that if the initialization is at  $x_0 < x_D$  while the aircraft is at  $x_T > x_D$ , the algorithm will converge to the false solution or to the negative-radical trap. Further, if the initialization uses  $x_0 < x_D$  but the positive sign of the radical in (5-3) or its equivalent in the partial-relaxation and rotated-coordinates algorithms is used, then the iteration will fall into the negative-radical trap. Finally, in any situation, initializing at  $x = x_D$  or a nearby value, or when the aircraft is near a tangency condition between the azimuth cone and the DME sphere, has a high probability of quickly entering the negative-radical trap.

In general, GS algorithms can be modified, or reconfigured, to converge correctly to the blue solution at the expense of incorrect behavior at the yellow.

Geometries with multiple solutions require that a GS PRA have a priori information to enable determining whether the solutions lie in one quadrant or two, and, in the latter case, which of the two is correct. As with the NR PRAs, this information is not available within the PRA, and must be provided externally. Approaches to resolving this difficulty are discussed in the next section.

It should be noted that the discussion of the GS PRAs was devoid of terms, central to the NR discussion in section 4, such as "singularity," and that the green and red solutions are almost totally disregarded. The GS principle does not rely on the notion of slope and gradient, or tangent to a surface, to form the next iterative estimate of location. Therefore, the question of singularities does not enter the discussion in this section; they have no place. And, as it is a near-zero gradient near a singularity that causes NR search to leap to a far-distant new estimate, its absence in the GS class precludes reaching such locations except by incomprehensibly bad initial conditions. The GS class has a different problem, handled by the negative-radical trap. In the circumstances involving this trap, the algorithm is attempting to search in a region where there is no real solution.

## SECTION 6

### RESOLVING THE MULTIPLE SOLUTIONS PROBLEM

The preceding sections have demonstrated that geometries with multiple solutions in coverage can exist in the MLS, that neither Newton-Raphson nor Gauss-Seidel PRAs can uniformly deal correctly with the problem, and that the information required to enable treating these situations correctly is not available within the MLS concept, but must be provided by some external means. This section considers various ways either to preclude the problem or to treat it by use of other sources of data.

#### 6.1 GROUND EQUIPMENTS

The problem of multiple solutions can be completely eliminated by new constraints on the siting of the ground units. Multiple solutions within coverage cannot occur in flight if the azimuth and elevation antennas are within the DME sphere; therefore, if the DME is closer to the azimuth antenna than to the elevation antenna there can never be more than two solutions (yellow and red in figure 6-1) to the geometrical problem, and only one solution (yellow) can be in coverage. The left side of this figure shows that the green and blue solutions of the quartic are complex in this geometry and are inaccessible to a real-valued PRA; the right side shows the geometry. It must be appreciated that this approach may require using one DME for each azimuth antenna, increasing the cost at some airports. This will be increased further if ground operations are expanded to enable steering, deceleration, and turnoff. Appendix B presents an alternate, and less restrictive but more complicated, principle for siting the DME so as to preclude multiple solutions in flight. In this context, see the discussion related to figure 6-2.

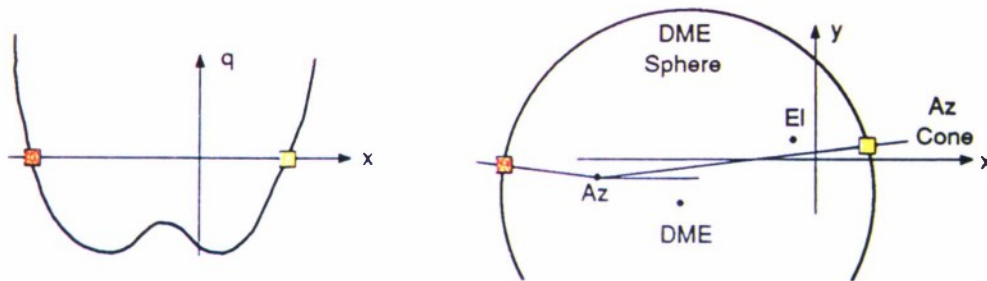


Figure 6-1. DME Site Constraint for One Solution in Coverage



The concept of the DME sphere for siting the DME relative to the azimuth and elevation antennas can easily be expressed in mathematical form. If the two conditions

$$\rho \geq \sqrt{(x - x_A)^2 + (y - y_A)^2 + (z - z_A)^2}$$

and

$$\rho \geq \sqrt{(x - x_E)^2 + (y - y_E)^2 + (z - z_E)^2}$$

are met, then there can be only one solution in coverage of both the azimuth and elevation antennas in flight operations. See, also, appendix B.

The planned uses for the MLS concept, in Cat III operation, include guidance of the aircraft on the ground after landing, so that steering, deceleration, and turnoff onto taxiways can be accomplished. This situation is somewhat simpler than the preceding, for the elevation antenna data and signals are irrelevant, and it is reasonable to assume that  $z_T = z_A = z_D = 0$  to an acceptable accuracy. In this case, it is possible to preclude multiple-solution geometries, which involve only the DME and the azimuth antenna, by locating the DME anywhere within the region marked "A" in figure 6-2. This region is characterized as a triangle with vertex at the azimuth antenna, and with vertex-angle  $2\alpha$ , where  $\alpha$  is determined by the maximum angle of the azimuth antenna,  $\theta_{MAX}$ , with  $\alpha = \pi/2 - \theta_{MAX}$ . This may be expressed as requiring  $y_D$  such that

$$|y_D - y_A| \leq |(x_D - x_A) \cot \theta_{MAX}|$$

This geometry is more restrictive of the DME siting than that suggested above, and is also more nearly conventional. It is valid for all range-sphere radii. This criterion could be used in the avionics to detect cases where the geometry is unsatisfactory for Cat III operation.

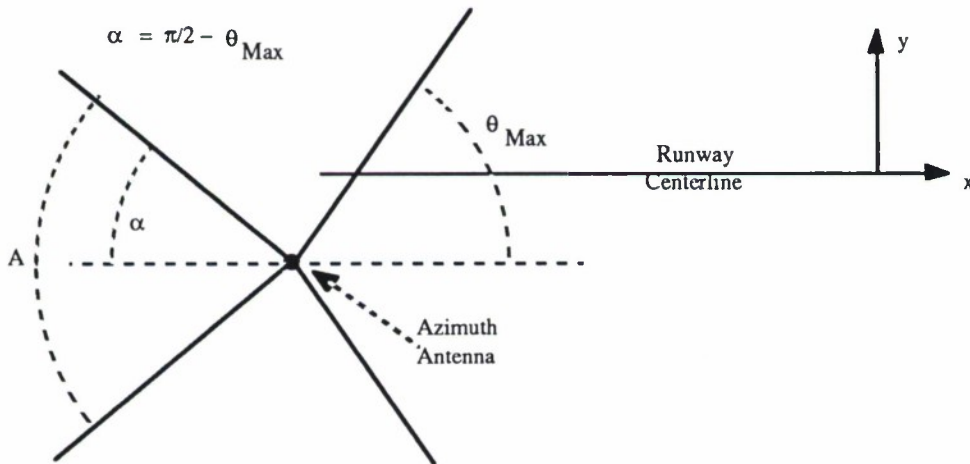


Figure 6-2. DME Sites for One Solution in Coverage on the Ground

It is important to appreciate that the problem of multiple solutions within coverage cannot happen with the Mobile Microwave Landing System (MMLS); this is true both for flight and ground operations. In the MMLS, the DME antenna is physically mounted on a bracket on the azimuth antenna, and the distance between the DME and the azimuth antenna is thus approximately zero. This condition is true even if the MMLS elevation antenna is collocated with the azimuth/DME combination.

## 6.2 AIRCRAFT FLIGHT PATHS

It is certainly possible to design pilots' airport instrument approach procedures so as to restrict the flight paths which may be used in RNAV with the MLS so that a multiple solutions geometry cannot occur within coverage. This may be the approach which airport operators will choose for fixed-base installations. To define such flight paths is outside the scope of this study. However, it may be remarked that such restrictions would tend to reduce the flexibility of ground unit siting and the curved, downwind, or dogleg approach trajectories, important and attractive features of the MLS concept.

## 6.3 AVIONICS

A variety of means may be used in the MLS avionics to preclude the multiple solutions situation, or to treat it correctly. Some of the potential solutions are now considered.

### 6.3.1 Avoidance

The principle implied in figure 6-1 may be used as the foundation for a method to avoid the multiple solutions situation. Thus, for example, if

$$\rho^2 \geq (x_D - x_A)^2 + (y_D - y_A)^2 + (z_D - z_A)^2 \quad (6-1)$$

then the azimuth antenna must be within the DME sphere. Further, since the elevation antenna cannot be upwind from the azimuth antenna, then it, too, must be within the DME sphere if the aircraft is receiving its signals. In this geometry, there is but one solution in coverage. Alternately, if

$$(x_D - x_A)^2 + (y_D - y_A)^2 + (z_D - z_A)^2 \leq (x_D - x_E)^2 + (y_D - y_E)^2 + (z_D - z_E)^2$$

then the DME is closer to the azimuth antenna than to the elevation antenna, and if the aircraft is in coverage, there is only one possible solution (yellow).

If neither of these conditions is satisfied, then the pilot cannot confidently use RNAV, for two solutions in coverage can exist in principle.

However, this approach does not preclude the multiple solutions problem, it merely mechanizes finding flight conditions which either do, or don't, have the problem. This

approach results in restricting the flight paths, or regions of the RNAV space, which may be used, and is thus subject to the objection that the system flexibility is reduced.

### 6.3.2 Position Data

It is possible to use position data provided by the Global Positioning System (GPS) to initialize either NR or GS PRAs. The civil GPS has degraded accuracy of about 100 meters (330'), the military GPS about 15 m (50'), and Differential GPS about 3 m (10'). But if the azimuth line-of-sight is nearly tangential to the DME sphere, even the military GPS will not guarantee the correct initial condition and correct solution, as shown in figures 4-7 and 4-8 for NR iteration. And similarly, that accuracy may not suffice for the required reconfiguration of a GS PRA, as discussed in section 5. If the geometry admits only one solution in coverage, then the accuracy of the civil GPS is more than adequate; but in this situation, the MLS itself contains enough information to initialize correctly.

### 6.3.3 Velocity Data

An alternate use of GPS has been suggested: use GPS to select an initial condition, and compare the velocity vector of the resulting solution to the GPS-derived velocity vector. This enables detection and rejection of the false solution or confirmation of the true solution; it does not provide any assistance in finding the true solution.

It was shown, in section 3, that the two solutions in coverage imply different velocity vectors. The velocity vector thus derived can be compared against the velocity vector measured from combining compass, airspeed, and perhaps winds-aloft data, to enable accepting or rejecting a proposed solution for aircraft location. This might not be sufficiently accurate near the tangency situation. However, velocity data derived from GPS or from an inertial navigation system (INS) should be satisfactory.

It is possible to use velocity data from very accurate sources to find the position solution in a multiple solutions geometry. Moreover, this approach can be used to determine, and thus correct, the error of the DME ( $\Delta\rho$ ). This approach, outlined below, implies a large increase in the magnitude, complexity, and computational burden of the avionics software.

Differentiate (2-1)-(2-3) with respect to time, and augment to include the DME error, to yield

$$(\rho_0 + \Delta\rho)\dot{\rho}_0 = (x - x_D)\dot{x}_0 + (y - y_D)\dot{y}_0 + (z - z_D)\dot{z}_0 \quad (6-2)$$

$$\dot{y}_0 = -[(x - x_A)\dot{x}_0 + (z - z_A)\dot{z}_0]\tan\theta_0/R_A - R_A\dot{\theta}_0\sec^2\theta_0 \quad (6-3)$$

$$\dot{z}_0 = [(x - x_E)\dot{x}_0 + (y - y_E)\dot{y}_0]\tan\phi_0/R_E + R_E\dot{\phi}_0\sec^2\phi_0 \quad (6-4)$$



where quantities with subscript o are to be interpreted as observation data provided from the MLS, and from the GPS or INS, as appropriate, rather than as initial values. The terms  $R_A$  and  $R_E$  were defined in (4-6) and (4-7). Given the observations of the angle, range, and velocity-component data, there must be only one solution for the unknowns,  $x$ ,  $y$ ,  $z$ , and  $\Delta\rho$ , which satisfies (6-2) through (6-4). However, there are only three equations at any instant and four unknowns, therefore several sets of observations spanning at least two distinct instants of time are required. Solution of this set of equations clearly is complicated. Several approaches are outlined.

### Full Kalman Filter

A Kalman filter PRA which takes into account all of the available information, including the aircraft maneuvers, can be formed. The description follows [7]. Define a state vector  $s$  as

$$\begin{aligned}s_1 &= \dot{x} \\ s_2 &= \dot{y} \\ s_3 &= \dot{z} \\ s_4 &= x \\ s_5 &= y \\ s_6 &= z \\ s_7 &= \Delta\rho\end{aligned}$$

Then the state-variable equation may be written

$$\dot{s} = F s + G \underline{w} + L \underline{u} \quad (6-5)$$

where  $\underline{w}$  is a vector of disturbances such as turbulence, with covariance matrix  $Q = E(\underline{w}\underline{w}^T)$ , and  $\underline{u}$  is a vector of control actions. The elements of the square matrix  $F$  are all zero except for  $F_{41} = F_{52} = F_{63} = 1$ . Note that  $F_{7i} = 0$  for all  $i$  to show that  $\Delta\rho$  is defined as a constant.

The matrix  $G$  is, similarly,  $7 \times 3$ , in which  $G_{11}$ ,  $G_{22}$ , and  $G_{33}$  are measures of the  $x$ -,  $y$ -, and  $z$ -direction components of disturbances such as turbulence, and the other elements are all small but non-zero. It is always good practice in Kalman filter design to assume some disturbances, even if none are known to be present; this protects the final result from imperfections in the assumed mathematical model.

The matrix  $L$  is  $7 \times 1$ ; it represents the accelerations produced in the several directions due to the control action  $\underline{u}$ , which is a vector function of the aircraft roll angle,  $\Phi$ , assumed to be provided to this vastly expanded KPRA. The elements of this matrix are

$$\begin{aligned}L_{11} &= -g\dot{\gamma}_0 \tan\Phi/V \\ L_{21} &= -g\dot{x}_0 \tan\Phi/V \\ L_{31} &= L_{41} = L_{51} = L_{61} = L_{71} = 0\end{aligned} \quad (6-6)$$



where  $V = \sqrt{\dot{x}_0^2 + \dot{y}_0^2}$  and it has been assumed that the aircraft turns in a coordinated manner and has a constant vertical velocity command. The aircraft roll angle  $\Phi$  is assumed to be positive if the right wing is down.

The state-variable "uncertainty covariance matrix,"  $P$ , satisfies the matrix Riccati differential equation

$$\dot{P} = FP + PF^T + GQG^T - K RK^T \quad (6-7)$$

where  $P$  is square and symmetric, and the differential equation is initialized as the uncertainty covariance matrix at  $t = 0$ ; the GPS or INS data may be used to provide these entries. Thus, if the civil GPS is used, then the main diagonal entries for  $P_{44}$  and  $P_{55}$  can be (100 meters)<sup>2</sup>.

The matrix Riccati differential equation for  $P$  given as (6-7) involves the Kalman gain matrix  $K$ , which is

$$K = PH^TR^{-1} \quad (6-8)$$

when the disturbances and measurement noise are uncorrelated. And this equation introduces two new matrices,  $R$  and  $H$ . The matrix  $R$  is the square, non-singular, measurement-noise covariance matrix, so that where  $\underline{y}$  is the measurement (or observation) noise,  $R = E(\underline{y}\underline{y}^T)$ .

The matrix  $H$  expresses the estimated observations in terms of the Kalman filter's state variables  $\underline{s}$ . These relationships may be deduced from (2-1)-(2-3) and (6-2)-(6-4).

The noise-contaminated observation error vector is  $\underline{z}$  where

$$\underline{z} = H\underline{s} + \underline{y} \quad (6-9)$$

The state estimation vector is

$$\dot{\hat{\underline{s}}} = F\hat{\underline{s}} + K(\underline{z} - H\hat{\underline{s}}) \quad (6-10)$$

The vector  $\hat{\underline{s}}$  is the least-squares optimal estimate of the vector  $\underline{s}$ . Its elements  $\hat{s}_4$ ,  $\hat{s}_5$ ,  $\hat{s}_6$ , and  $\hat{s}_7$  are the continuous-time domain estimates for  $x$ ,  $y$ ,  $z$ , and  $\Delta\rho$ , respectively.

### Simple Kalman Filter

A simple Kalman filter can be devised. This approach uses as the state vector  $(s_1 \ s_2 \ s_3 \ s_4)^T = (x_0 \ y_0 \ z_0 \ \Delta\rho)^T$ , with only four states, assumed to be constants from an initial assumption. Then form

$$\begin{aligned}
x &= x_0 + \int \dot{x}_0 dt \\
y &= y_0 + \int \dot{y}_0 dt \\
z &= z_0 + \int \dot{z}_0 dt \\
\rho &= \rho_0 + \Delta\rho
\end{aligned}
\tag{6-11}$$

Using (6-11) and the observations (2-1)-(2-3), form estimates of  $\rho$ ,  $\theta$ , and  $\phi$ , etc.

The state matrix  $F$  is a 4x4 square matrix, with all elements equal to zero, to embody the assumption that the several variables are all unknown constants. The rest of the development follows the outline offered above. A typical layout for Kalman filters is shown in figure 6-2. It must be appreciated that even this rather simple Kalman filter entails complexity far greater than the PRAs which are envisioned for MLS avionics.

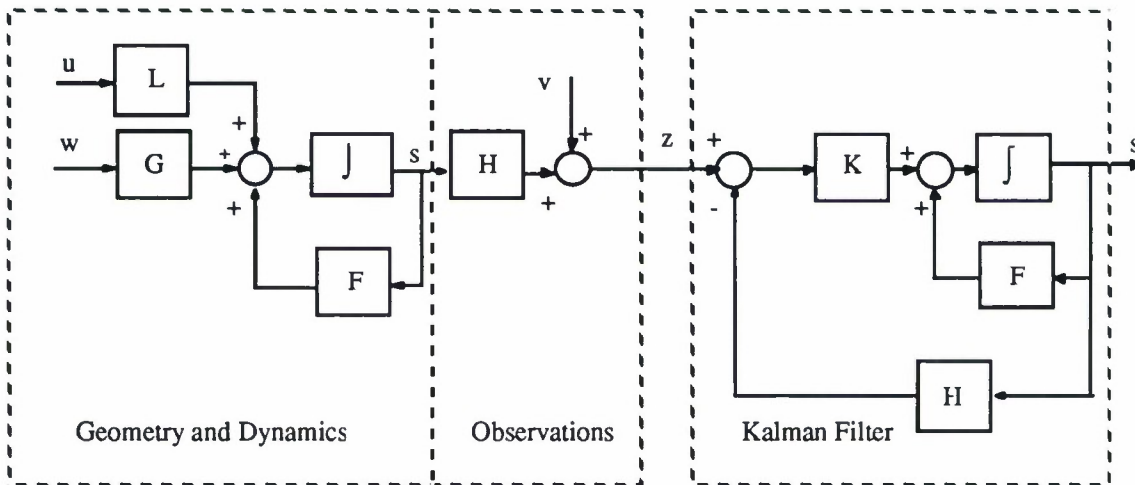


Figure 6-3. Kalman Filter for Multiple Solutions

In this approach, it is essential to assume a larger disturbance covariance matrix than before, for the assumption that the state vector components are constants is clearly unsound, due to aircraft maneuvers.

#### Adaptive Technique

Adaptive techniques, described in references 8, 9, and 10, can be used effectively. Use the approach described in (6-11) to form estimates of  $x$ ,  $y$ ,  $z$ , and use (2-1)-(2-3) to define estimates of the observations. Compare these estimates to the actual observations to

$$\begin{aligned}
\varepsilon_1 &= \theta_o - \theta \\
\varepsilon_2 &= \phi_o - \phi \\
\varepsilon_3 &= \rho - \rho_{T'}
\end{aligned}
\tag{6-12}$$

form error terms where the hats denote the estimates of the observations, and the subscripts o define the measured observations, as before, and  $\rho_{T'}$  is the estimated true slant range,  $\rho_{T'} = \rho_o + \Delta\rho$ .

An adaptive, steepest descent, gradient algorithm such as

$$\begin{aligned}
\dot{x} &= -K_x \partial \varepsilon_3^2 / \partial x \\
\dot{y} &= -K_y \partial \varepsilon_1^2 / \partial y \\
\dot{z} &= -K_z \partial \varepsilon_2^2 / \partial z \\
\Delta\rho &= -K_\rho \partial \varepsilon_3^2 / \partial \Delta\rho
\end{aligned}
\tag{6-13}$$

will enable convergence to the correct solutions. It should be noted that (6-13) has a fundamental similarity to the NR approach. However, consider the implications of figure 3-4, expanded to include two separate instants, in the context of the implications of figure 3-6. It is probable that there is no geometry of ground sites and aircraft location for which a unique aircraft velocity permits more than one solution. In this case, the unknowns on the left of (6-14) can be arbitrarily initialized, a property of NR problems which have only one solution. The gains  $K_x$ ,  $K_y$ ,  $K_z$ , and  $K_\rho$  must all be positive, and should have values such that the rates of convergence of the unknowns on the left in (6-14) towards the solution are of the order of 500 feet/second if the variables are initialized to the estimates of position provided by the GPS, or to 1000 or 2000 feet/second if the MLS is used to initialize the variables.

Pilot

If the two velocity vectors which the two solutions generate were exposed to the pilot, he (or she) would normally have little difficulty in selecting the correct solution. This approach would involve relatively little complexity; however, it involves the possibility of confusing the pilot, especially in a near-tangency situation.

#### 6.3.4 A Philosophical Comment

To a large extent, these Kalman and adaptive approaches contradict the fundamental philosophy of the MLS concept: the observations of range, and of the azimuth and elevation angles, should be so accurate that sophisticated filtering techniques should not be required.

## 6.4 OVERVIEW

There appear to be three ways to deal with the multiple solutions problem:

- a. Restrict the siting arrangements of the ground equipments to preclude these geometries,
- b. Restrict the pilot's approach procedures for the aircraft flight paths to be allowed so that such geometries cannot properly occur, and,
- c. Enable the avionics to exclude or to handle these situations correctly.

The second approach is viewed as undesirable, for restricting the flight paths reduces the flexibility of the MLS concept, which is one of its major attractions. Similarly, the avionics integration, and the complicated algorithms required to implement solution of the problem, are expensive, and contradict the philosophy of high accuracy signals and data on which the MLS concept is based. It is therefore considered that the most appropriate and least expensive way to avoid the problem of multiple solution geometries is to preclude them by appropriate siting restrictions of the ground units. However, the proposed siting constraints might require additional DME units at some airports, or restriction of the flight paths allowed for aircraft at these airports.



## SECTION 7

### CONCLUSIONS

1. In normal or collocated configurations of the three ground units there is only one solution for aircraft location within the MLS coverage volume, and there is no special difficulty in devising algorithms, including the requisite initialization thereof, that will reliably converge to that unique solution.
2. The current siting rules of reference 1 were designed to accept a few preexisting installations with unconventional geometries. However, these rules should not be interpreted as encouraging unconventional arrangements. Some unconventional geometries, which are within the constraints as presently constituted, permit multiple solutions for aircraft location within the system coverage. When multiple solutions exist within coverage, the MLS cannot internally determine which is correct; this essential information, or the equivalent, must be provided from another source.
3. If, for all values of aircraft distance from the DME, both the azimuth and elevation antennas are within the DME sphere, then there can be only one possible solution for aircraft location within the MLS coverage. Therefore, multiple solutions cannot occur with the MMLS, because the azimuth antenna and the DME are always and inevitably collocated due to their physical arrangement.
4. Multiple solutions geometries can be precluded by new restrictions on the allowable siting of the ground units for installations in the future. In particular, the location of the DME relative to the azimuth antenna is critical. This is viewed as the preferred approach
5. The multiple solutions problem can also be precluded by suitable design of pilot approach procedures for each airport. However, this may reduce the flexibility of allowable RNAV operations at the airport. Further, if the pilot should by error fly into a region where a false solution exists, and the MLS avionics should either track the false solution, or be unable to track the true solution, then the potential for an accident exists. Nonetheless, this may be the appropriate way to deal with the preexisting installations with unconventional geometries.
6. The multiple solutions problem can be handled successfully by modifications in the avionics. However, these modifications reduce the flexibility and utility of the MLS concept, or involve significant added complexity and cost, due to the integration with other avionics which would be required, and also due to the very large size and computational burden of the new algorithms which would be required. The alternate, requiring the pilot to select the correct solution, involves the probability of confusing the pilot. This approach is therefore not recommended.

## LIST OF REFERENCES

1. International Civil Aeronautic Organization, April, 1985, with corrections of 22 October, 1987, *International Standards, Recommended Practices and Procedures for Air Navigation Services; Aeronautical Telecommunications*, Annex 10, Fourth Edition.
2. *Minimum Operational Performance Standards for MLS Area Navigation Equipment*, March 18, 1988, Document No. RTCA/DO-198, Appendix D, prepared by SC-151, Radio Technical Commission for Aeronautics, Washington, D. C.
3. *Introduction to MLS*, October, 1987, United States Department of Transportation, Federal Aviation Administration, Washington, D. C.
4. Hall, J. W., P. M. Hatzis, and F. D. Powell, July 1990, *Examination of RTCA/DO-198 Position Reconstruction Algorithms for Area Navigation with the Microwave Landing System*, ESD-TR-90-308, AD A224 804, Electronic Systems Division, Hanscom Air Force Base, MA.
5. Hall, J. W., P. M. Hatzis, and F. D. Powell, July 1990, *A Gaussian Algorithm Using Coordinate Rotation for Area Navigation with the Microwave Landing System*, ESD-TR-90-315, AD A225 642, Electronic Systems Division, Hanscom Air Force Base, MA.
6. Hatzis, P. M., and F. D. Powell, November 1990, *A Successive Partial-Relaxation Gaussian Algorithm for Area Navigation with the Microwave Landing System*, ESD-TR-90-326, AD A228 871, Electronic Systems Division, Hanscom Air Force Base, MA.
7. Gelb, A., ed., 1974, *Applied Optimal Estimation*, The Analytical Sciences Corp., M. I. T. Press, Cambridge, MA.
8. Powell, F. D., June 1970, *Adaptive Modelling and Control*, Bell Aerospace Co. Report No. 9500-920183, Final Report on Office of Naval Research, Information Sciences Branch, Contract Nonr-4864(00), NR049-207.
9. Eyckhoff, P., October 1963, Aspects of Process Parameter Estimation, *IEEE Transactions on Automatic Control*.
10. Narendra, K. S., and L. E. McBride, October 1963, Multi-Parameter Self-Optimizing System Using Correlation Techniques, *IEEE Transactions on Automatic Control*.

## APPENDIX A

### SECONDARY SOLUTIONS USING TRACKING FILTERS

Assume that the PRA has found the unique correct primary solution, perhaps by the methods discussed in section 6, and that the process for finding the correct primary solution is sufficiently complicated that it should, if possible, not be repeated. Assume, further, that the PRA has been tracking that solution successfully for a short interval, one or two seconds. This appendix examines the potential uses of this information to enable maintaining track on this solution, even in situations where the true and a false solution interchange their roles or properties. In turn, the techniques useful for maintaining track of the correct solution are valuable as part of the technique for finding the primary solution.

Algorithms for establishing secondary solutions are outlined below. It should be noted here that these algorithms may be applied to any situation in which minimum-lag filtering of a signal is desired, or in which tracking and/or prediction or coasting are required. Further, these techniques can:

- a. Minimize the number of iterations required to reach a stable solution;
- b. Minimize errors of estimated position due to noise in the observations;
- c. Enable use of DME data in back-azimuth operation;
- d. Enable passing through a transition between regions where true and false solutions interchange roles and locations;
- e. Estimate the rate of a signal, and thus,
- f. Enable "coasting" in the absence of received MLS signals and
- g. Enable synchronizing angular and range data.

Tracking filters with these properties may be invariant or adaptive, and in finite or infinite impulsive-response forms.

#### A.1 INVARIANT TRACKERS

Time-invariant trackers with finite and with infinite impulsive-response (FIR and IIR, respectively) forms are now described.

### A.1.1 Finite Impulsive Response Filter

An algorithm is presented which provides coasting, synchronism, and Least Square Error (LSE) performance for all three data types or aircraft location components. This time-invariant filter estimates position of a variable at the present instant by using an internally generated estimate of the rate of that variable. The rate information can therefore be used for coasting or synchronizing, as required.

The principles of this filter are outlined. Assume that the variable (an angle, or range, or a component of position estimate) is approximated as

$$X_i = a + bt_i \quad (\text{A-1})$$

where

$X_i$	Estimate of variable at instant $i$
$a, b$	Unknown coefficients, to be estimated to an LMSE criterion
$\xi_i$	Measured variable-datum at instant $t_i$
$i$	Index, $i = 0, 1, 2, \dots, n$
$t_i$	Times of observations, in the past so that $i = 0$ is the present or most recent, and $i = n$ is the most-distant past

At each instant  $i$  the approximation (A-1) has an error  $\epsilon_i = X_i - \xi_i$  so that there is a sequence of  $n$  observations and errors of the form

$$\begin{pmatrix} \epsilon_0 \\ \epsilon_1 \\ \vdots \end{pmatrix} = \begin{pmatrix} 1 & t_0 \\ 1 & t_1 \\ \dots & \end{pmatrix} \begin{pmatrix} \xi_0 \\ \xi_1 \\ \vdots \end{pmatrix} \quad (\text{A-2})$$

with  $i = 0, 1, 2, \dots, n$ . The coefficients  $a$  and  $b$  are unknown, and are to be determined to a least square error criterion. Premultiplying (A-2) by the transpose of the  $2 \times n$  matrix in (A-2) yields the matrix equation which embodies the least square error values for  $a$  and  $b$  as

$$\begin{pmatrix} n+1 & \Sigma t_i \\ \Sigma t_i & \Sigma t_i^2 \end{pmatrix} \begin{pmatrix} a \\ b \end{pmatrix} = \begin{pmatrix} \Sigma \xi_i \\ \Sigma \xi_i t_i \end{pmatrix} \quad (\text{A-3})$$

with solution, where  $m = n + 1$ ,

$$\begin{pmatrix} a \\ b \end{pmatrix} = \begin{pmatrix} \Sigma t_i^2 & -\Sigma t_i \\ -\Sigma t_i & m \end{pmatrix} \begin{pmatrix} \Sigma \xi_i \\ \Sigma \xi_i t_i \end{pmatrix} / [m \Sigma t_i^2 - (\Sigma t_i)^2] \quad (\text{A-4})$$

and the estimate of the variable  $X$ , where  $\tau$  is the interpolation or prediction interval, is

$$X = a + b\tau = [(\Sigma t_i^2 \Sigma \xi_i - \Sigma t_i \Sigma t_i \xi_i) + \tau(m \Sigma t_i \xi_i - \Sigma t_i \Sigma \xi_i)] / [m \Sigma t_i^2 - (\Sigma t_i)^2] \quad (\text{A-5})$$



The properties of (A-5) are considered. If  $\tau < 0$ , the filter produces lag, or interpolation into the past. If  $\tau = 0$  (when corrected for the delay between the most recent datum and the present instant) then we have a zero-lag filter which estimates the present value of the variable to LMSE accuracy, given the noise actually present in the system. And if  $\tau > 0$ , the filter provides extrapolation into the future; this may be used as desired for synchronizing, for coasting, or for finding another secondary initialization which will be as close as possible to the correct solution. Finally, the rate parameter,  $b$ , will be used in selecting the correct primary setup, in section 5. These properties hold if the input is constant or a ramp in time, or a constant plus a ramp. Such inputs are reasonable approximations to the flight of an aircraft over short intervals of time.

Note that the oldest datum, at  $t = t_n$ , determines the time-constant of this filter and should therefore be small enough so that maneuvers by the aircraft do not contaminate the result. In the MLS application,  $t_n = 2$  seconds is considered appropriate, as that is shorter than the maneuver or turbulence response times of an aircraft in landing approach, but is long enough to provide a useful degree of averaging and thus reduction of noise in the data,  $\xi_i$ .

Table A-1 shows the behavior of this filter. The first two lines of this table present the various values of the index  $i$  and the corresponding values of time, assumed to be at uniform intervals of 0.2 seconds in the past. There are 11 instants spanning 2.0 seconds. The third line shows the history of the input signal  $\xi_i$ , which is the combination of a step with a ramp having a rate of -5 units per second. The two lines below show the calculated values for the coefficients  $a$  and  $b$ . The coefficients  $a$  and  $b$  converge at and after the second instant ( $i = 9$ ) to the correct values ( $a = X = \xi = 10$  and  $b = \text{rate} = -5$ ) for the instant  $t = \tau = 0$ , as desired. Notice that data have been used only at intervals of 0.2 seconds, whereas the angle data are available at intervals of  $1/39 = 25.6$  milliseconds; any error in the coefficients due to noisy data can therefore be attenuated by approximately the factor  $\sqrt{5/39} = 0.36$  if desired or required.

**Table A-1. Performance of a Time-Invariant FIR Filter**

Index, $i$	10	9	8	7	6	5	4	3	2	1	0
Time, $t_i$	-2.0	-1.8	-1.6	-1.4	-1.2	-1.0	-0.8	-0.6	-0.4	-0.2	0.0
Input, $\tau_i$	20	19	18	17	16	15	14	13	12	11	10
a		10	10	10	10	10	10	10	10	10	10
b		-5.0	-5.0	-5.0	-5.0	-5.0	-5.0	-5.0	-5.0	-5.0	-5.0

### A.1.2 An Infinite Impulsive Response Filter

An IIR filter, equivalent in principle to the FIR filter described above and with the same features and uses, is now described; see figure A-1. The input to this filter may, as with the FIR filter discussed in the preceding subsection, be angular, DME, GPS data, or a raw reconstructed position component. The output is the least squared error filtered estimation for a  $\tau$ -second prediction ( $\tau > 0$ ) of the same variable, under the assumption that the input is essentially a constant plus a ramp in position component. As before, this assumption is valid if the filter's time-constant is of the order of two seconds. If the filter is invariant, then for the MLS application, the loop gain (a) should yield a half-period of somewhat less than 2 seconds, so that  $a = \pi^2/2$  (radians/second)<sup>2</sup>, while the feedback (b) should yield a damping-ratio of approximately  $1/\sqrt{2}$ .

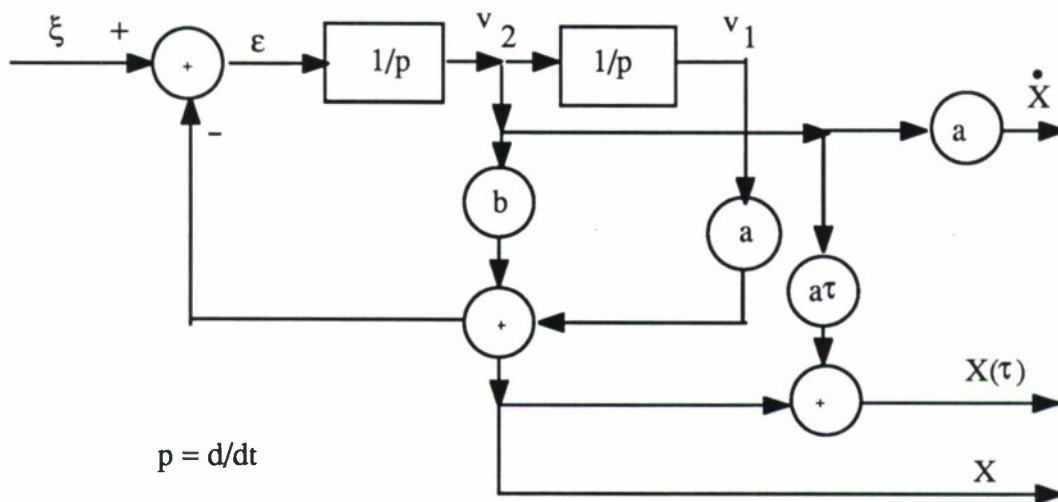


Figure A-1. An IIR Tracker

The output is the least squared error filtered estimation for a  $\tau$ -second prediction (if  $\tau > 0$ ) of the same variable, under the assumption that the input is essentially a constant plus a ramp in time.

Table A-2 shows the response of this filter to be the same time history used in table A-1, i. e., a combination of a step and a ramp. The state variable is initialized at the measured input value of  $\xi = 20$  at  $t = 0$ . The time and index-number count positively from zero, as this is a time-domain filter, opposite to the principle for the FIR filter of the preceding subsection. The input, in the third row, is identical to that in table A-1. The output estimate,  $X$ , is shown in the fourth row; as time approaches two seconds, the filter output follows the input very closely, so that its output rate-variable is also an accurate estimator of the rate.

The last row of table A-2 shows a 2-second prediction of the input and output; this should ideally be  $-5 \times 2 = -10$  units (below) the input. This requirement is approximately satisfied for time greater than 1.4 seconds after startup.

The IIR filter has some advantages over the FIR type which should be noted. The principal advantage is that it requires only two memory registers. A second advantage, which is discussed in the next subsection, is that it can become an adaptive unit relatively easily.

**Table A-2. Performance of a Time-Invariant FIR Filter**

Index, $i$	0	1	2	3	4	5	6	7	8	9	10
Time, $t_i$	0.0	0.2	0.4	0.6	0.8	1.0	1.2	1.4	1.6	1.8	2.0
Input, $\xi_i$	20	19	18	17	16	15	14	13	12	11	10
Output, $X$	20	19.8	19.1	18.1	16.9	15.7	14.4	13.2	12.1	11.0	10.0
$\tau = 2$ sec. prediction	20	19.1	16.6	13.4	10.3	7.5	5.1	3.2	1.7	0.5	-0.6

## A.2 ADAPTIVE TRACKERS

Section A.1 presented FIR and IIR tracking nets. In this subsection, the use of adaptive principles to improve the performance of such trackers is considered.

The trackers shown in section A.1 are time-invariant, and their structure does not permit taking advantage of new data to improve their performance. Conversion to adaptive forms enables adjustment to treat optimally situations in which the spectra of noises in the measurements differ from those assumed a priori, or the disturbances such as gusts or maneuvers are more (or less) important than assumed.

### A.2.1 Adaptive FIR Trackers

It is possible to make an adaptive tracker in a FIR form, but it is inefficient to do so. An adaptive tracker in the form used in section A.1.1 could be realized by separately weighting each datum-element,  $\xi_i$ , in (A-2) with an individual adaptive weight,  $g_i$ , so that (A-2) takes the form

$$\begin{pmatrix} \epsilon_0 \\ \epsilon_1 \\ \vdots \end{pmatrix} = \begin{pmatrix} 1 & t_0 \\ 1 & t_1 \\ \vdots & \vdots \end{pmatrix} \begin{pmatrix} a \\ b \end{pmatrix} - \begin{pmatrix} g_0 \xi_0 \\ g_1 \xi_1 \\ \vdots \end{pmatrix} \quad (\text{A-6})$$

But it immediately becomes evident that there must be as many adaptive weights ( $g_i$ ) as there are elements of data in the memory-registers. This very rapidly becomes unacceptably inefficient. This approach is thus unsuited to the need and is abandoned.

### A.2.2 An Adaptive IIR Tracker

Figure A-1 may be modified to be adaptive, as shown in references A-1, A-2, and A-3. The objective of the filter is to produce an output signal which is, not at each instant but in the average, as much like the average or mean of the input as possible. Then a valid Index of Performance to be minimized is the integral over time of the square of  $\epsilon$ , and the adjustable parameters are the gains  $a$  and  $b$  in figure A-1. The theoretical foundations follow.

The transfer function which defines the error  $\epsilon$  as a function of the input time-history  $\xi$  is

$$\epsilon = [p^2 / (p^2 + bp + a)]\xi \quad (\text{A-7})$$

where  $a$  and  $b$  are gains, to be adapted, and  $p$  is a time-differential operator so that  $(1/p)$  may be viewed as an integration.

Define an index of performance, to be minimized, as

$$J = \int \epsilon^2 dt \quad (\text{A-8})$$

Then an adaptation rule for least mean square error performance is

$$\begin{aligned} \dot{a} &= -k_a \left( \frac{\partial J}{\partial a} \right) = -2k_a \epsilon (\partial \epsilon / \partial a) \\ \dot{b} &= -k_b \left( \frac{\partial J}{\partial b} \right) = -2k_b \epsilon (\partial \epsilon / \partial b) \end{aligned} \quad (\text{A-9})$$

where  $k_a$  need not equal  $k_b$  but both must be positive and small enough to produce averaging so that the least-square minimum is achieved when

$$\begin{aligned} \bar{\dot{a}} &= -k_a \left( \overline{\frac{\partial J}{\partial a}} \right) = -2k_a \overline{\epsilon (\partial \epsilon / \partial a)} = 0 \\ \bar{\dot{b}} &= -k_b \left( \overline{\frac{\partial J}{\partial b}} \right) = -2k_b \overline{\epsilon (\partial \epsilon / \partial b)} = 0 \end{aligned} \quad (\text{A-10})$$



where the overbars imply time-averaging. Notice that if  $k_a$  and  $k_b$  are too large,  $\epsilon$  approaches zero at all instants of time but the intent to average is defeated; it is essential that these gains be small and produce averaging, as shown in (A-10).

Substituting (A-7) into (A-9) and partially differentiating yields

$$\partial \dot{J} / \partial a = -[1/(p^2 + bp + a)]\epsilon$$

and

$$\partial \dot{J} / \partial b = -[p/(p^2 + bp + a)]\epsilon$$

(A-11)

Figure A-2 shows a filter which generates these terms, and thus produces continuously adapting values of the gains  $a$  and  $b$ , which are to be used in both nets, figures A-1 and A-2. As noted, the input to the circuit of figure A-2 is the error-term,  $\epsilon$ , from figure A-1. It may be remarked that this type of tracker is related to the concept of an  $\alpha$ - $\beta$  tracker.

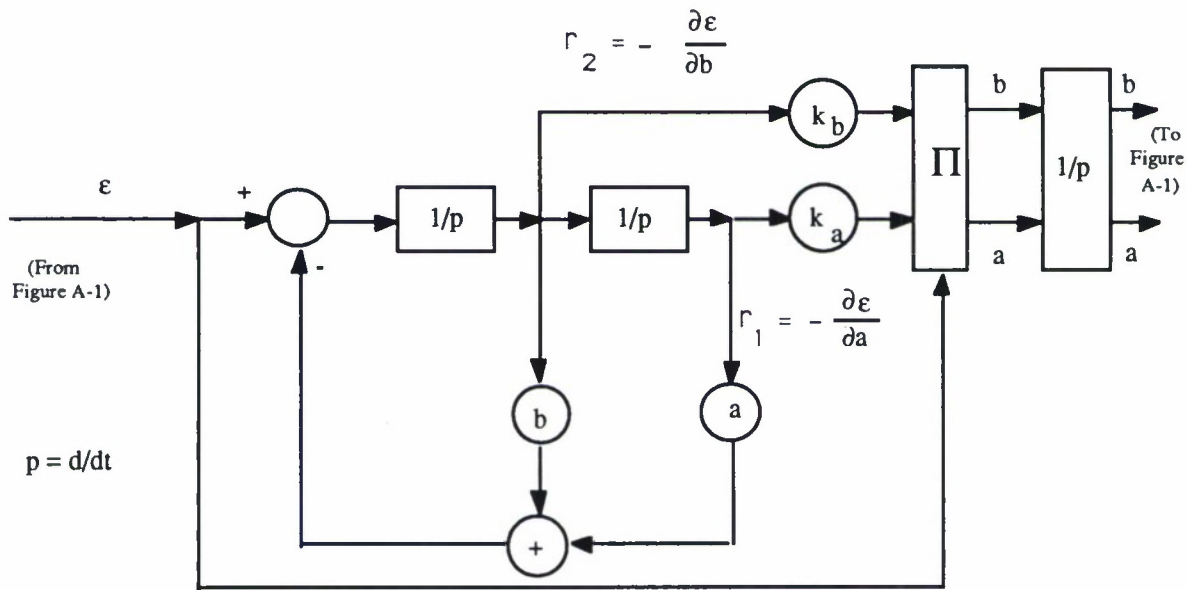


Figure A-2. Adaptive Filter

With either the adaptive or the invariant filter approach, it is possible to form an estimate for any of the variables of measurement or of the components of position estimate to

use as an initial condition with accuracy sufficient to preclude the possibility of the PRA converging to a false solution, to synchronize the observed data if necessary, to maintain an up-to-date estimate of position during an interval of loss of signal (coasting), or to use during a back-azimuth operation.

These filters, and especially their rate-estimating capability, may be used as the theoretical and practical foundation for developing the Kalman or other initialization algorithms developed in section 6. However, see again the philosophical comments in section 6.3.4; their point was that the inherent and fundamental MLS accuracy should be such that Kalman filtering should not be required.

## LIST OF REFERENCES

- A-1. Gelb, A., ed., 1974, *Applied Optimal Estimation*, The Analytical Sciences Corp., M. I. T. Press, Cambridge, MA.
- A-2. Powell, F. D., June 1970, *Adaptive Modelling and Control*, Bell Aerospace Co. Report No. 9500-920183, Final Report on Office of Naval Research, Information Sciences Branch, Contract Nonr-4864(00), NR049-207.
- A-3. Eyckhoff, P., October 1963, *Aspects of Process Parameter Estimation*, IEEE Transactions on Automatic Control.





## APPENDIX B

### GENERAL SITING CONSTRAINTS FOR THE DME

The concept of the DME sphere has been used throughout this report. This concept is that if the DME site and the aircraft position are such that the DME sphere, with center at the DME and radius from the DME to the aircraft, contains both the azimuth and the elevation antennas, then multiple solutions cannot exist within coverage. This concept is here expanded to include the further condition that this be true for any DME sphere, i.e., a sphere of any radius; this new condition creates a criterion that does not depend on the position of the aircraft. The former condition merely states that there can be but one solution in coverage for the particular range at that instant; this may be useful to enable avionics to detect geometries where multiple solutions can exist, as noted above. But that approach does not treat the problem for all instants, nor for all ranges and aircraft locations. This topic is now considered, rephrased as, "What sites for the DME can never have more than one solution in coverage, independent of the location of the aircraft?" The demonstration is restricted to the assumptions that the ground equipments are all at ground altitude, and that the aircraft altitude is so low that it can be neglected. This is not a severe restriction, as the elevation antenna proportional coverage extends only to about  $15^\circ$ . Note that the DME sphere becomes the DME circle under this assumption.

The general problem may be divided into two configurations, exclusive and inclusive. In the exclusive configuration, the elevation antenna is outside the region of coverage of the azimuth antenna; in the inclusive configuration, the elevation antenna is within that coverage. The two cases are considered in order; the argument is geometric.

Consider figure B-1, showing an exclusive configuration, with the azimuth and elevation antennas on opposite sides of the runway, and with rather little x-direction distance between them. This configuration is related to Case 2 of sections 3 through 5. The azimuth coverage is contained within the region ABC; the elevation horizontal plane coverage is in the region DEF. The region of coverage by both antennas is to the right of the DGHF boundary. A line, marked IHG is orthogonal to the azimuth line of sight AHB at the edge of coverage at H. If the DME is on (or to the left of) the line segment IH, any DME circle that has a segment in the elevation coverage region has only one possible azimuth intercept, and thus only one solution in coverage. Assume the DME site is anywhere exactly on the line-segment IH; then the azimuth antenna site at B is interior to any arc which is within the joint coverage region, for such an arc is orthogonal to IG at their intersection. The same argument holds, symmetrically, if the DME is on, or to the left of, the line-segment HG; however, for this option, the DME site is in the BHG region. In either of these situations a DME circle can be drawn that contains neither of the antennas, and a DME circle can also be drawn that contains only one antenna; in each case there is only one solution in coverage. This demonstrates that the concept of the DME sphere is sufficient but not necessary as a condition for only one solution in coverage, and that more general conditions can be proposed.

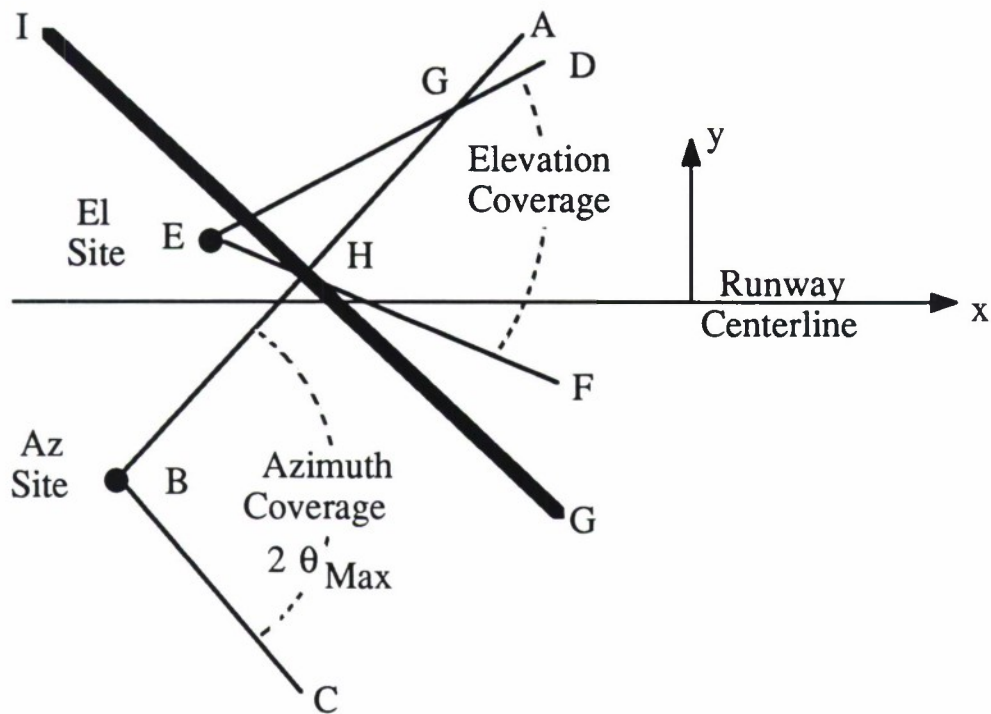


Figure B-1. DME Sites for an Exclusive Geometry

Figure B-2 shows the inclusive geometry, where the elevation antenna is within the coverage of the azimuth antenna. This is more nearly a conventional arrangement, and is related to Case 1, discussed in sections 3 through 5. For this geometry, draw a line from the azimuth antenna site to the elevation antenna site, and erect a perpendicular to that line at the elevation antenna site. If the DME is on or to the left of this line, IG, there can be only one solution in coverage. Again, this condition can be satisfied with neither antenna or only one antenna within the DME circle, and it is thus a more general condition than the DME circle concept offers.

The discussion in section 6 covers the case of Cat III operation on the ground, when the siting of the DME involves only the coverage of the azimuth antenna. This discussion need not be repeated here.

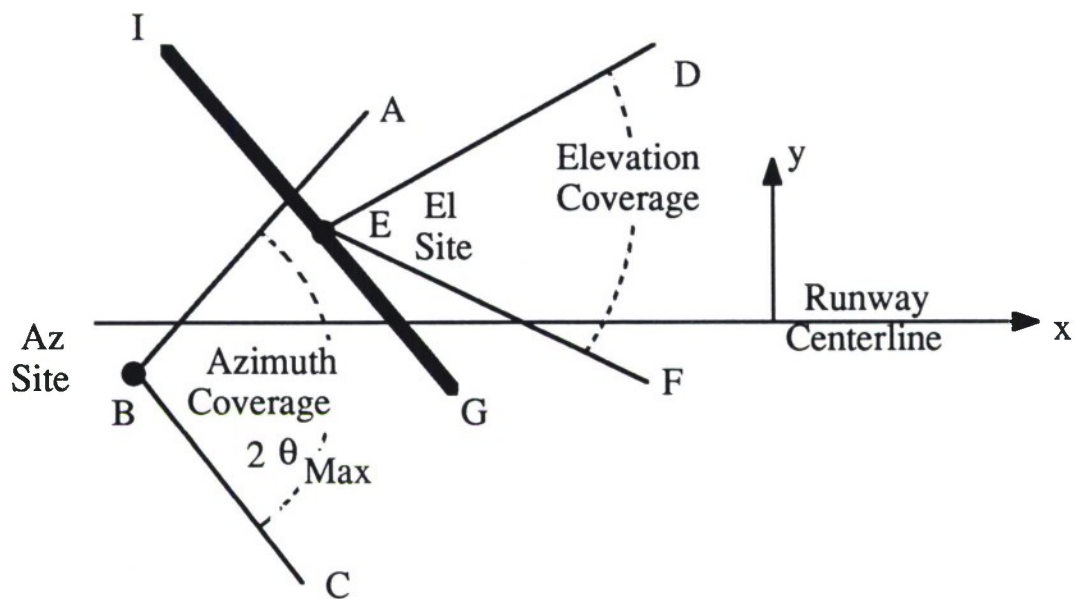


Figure B-2. DME Sites for an Inclusive Geometry

## GLOSSARY

<b>Az</b>	Azimuth Antenna
<b>Cat</b>	Category
<b>DME</b>	Distance Measuring Equipment Transponder
<b>El</b>	Elevation Antenna
<b>FIR</b>	Finite Impulsive Response
<b>GPS</b>	Global Positioning System
<b>GS</b>	Gauss-Seidel
<b>ICAO</b>	International Civil Aeronautics Association
<b>IIR</b>	Infinite Impulsive Response
<b>LSE</b>	Least Square Error
<b>MLS</b>	Microwave Landing System
<b>MMLS</b>	Mobile Microwave Landing System
<b>NR</b>	Newton-Raphson
<b>PRA</b>	Position Reconstruction Algorithm
<b>RGS</b>	Rotational Gauss-Seidel
<b>RNAV</b>	Area Navigation
<b>SPR</b>	Sequential Partial Relaxation



